Cell Reports

Article

MDA-LDL vaccination induces athero-protective germinal-center-derived antibody responses

Graphical abstract

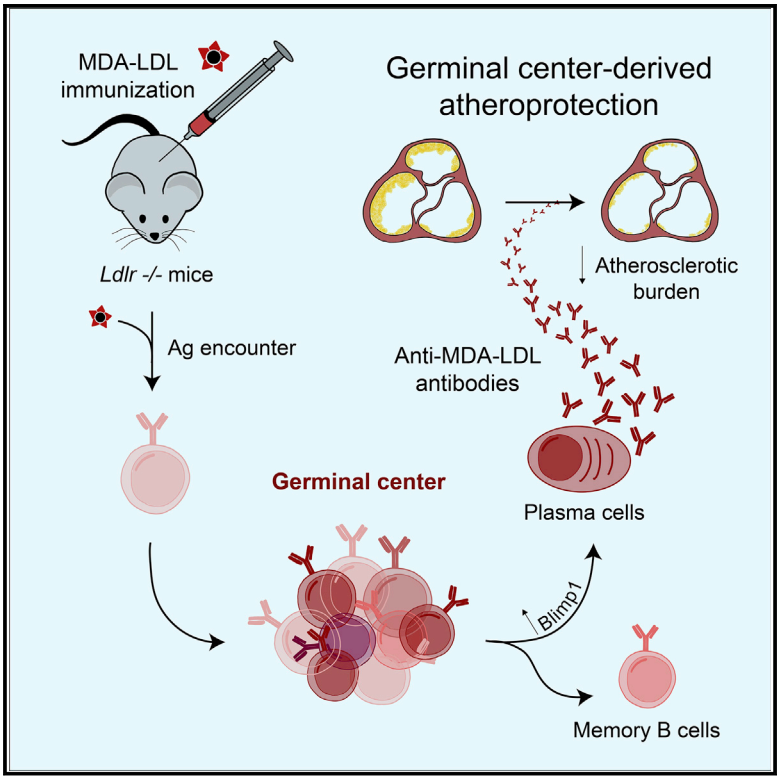

Highlights

- MDA-LDL immunization triggers a GC response
- Pro-atherogenic mice deficient for GC-derived PCs show accelerated atherosclerosis
- MDA-LDL-driven athero-protection is impaired in mice lacking GC-derived PCs

Authors

Inmaculada Martos-Folgado, Alberto del Monte-Monge, Cristina Lorenzo, ..., Jose L. Martín-Ventura, Hedda Wardemann, Almudena R. Ramiro

Correspondence

aramiro@cnic.es

In brief

Martos-Folgado et al. show that immunization with MDA-LDL elicits a GC-derived antibody immune response. Furthermore, the authors demonstrate that GC-derived antibodies drive MDA-LDL-induced athero-protection. These results uncover the mechanism underlying MDA-LDL-driven athero-protection and support the development of MDA-LDL-based vaccines for the prevention or treatment of atherosclerosis.

Martos-Folgado et al., 2022, Cell Reports *41*, 111468
October 11, 2022
https://doi.org/10.1016/j.celrep.2022.111468

CellPress

Cell Reports

CellPress
OPEN ACCESS

Article

MDA-LDL vaccination induces athero-protective germinal-center-derived antibody responses

Inmaculada Martos-Folgado,[1,2] Alberto del Monte-Monge,[1] Cristina Lorenzo,[1] Christian E. Busse,[3] Pilar Delgado,[1,9] Sonia M. Mur,[1] Laura Cobos-Figueroa,[1,4,10] Joan C. Escolà-Gil,[5,6] Jose L. Martín-Ventura,[7,8] Hedda Wardemann,[3] and Almudena R. Ramiro[1,11,*]

[1]B Lymphocyte Biology Lab, Centro Nacional de Investigaciones Cardiovasculares (CNIC), Madrid, Spain
[2]Medical Department, Pfizer S.L.U., Madrid, Spain
[3]Division of B Cell Immunology, German Cancer Research Center, Heidelberg, Germany
[4]Grupo de Manufactura Avanzada con Láser del Centro Láser (UPM), Madrid, Spain
[5]CIBER de Diabetes y Enfermedades Metabólicas Asociadas (CIBERDEM), Madrid Spain
[6]Institut de Recerca de l'Hospital de La Santa Creu I Sant Pau, Barcelona, Spain
[7]CIBER de Enfermedades Cardiovasculares (CIBERCV), Madrid, Spain
[8]Vascular Pathology Lab, IIS-Fundación Jiménez Díaz-Universidad Autónoma, Madrid, Spain
[9]Present address: Centro de Biología Molecular Severo Ochoa, Consejo Superior de Investigaciones Científicas, Universidad Autónoma de Madrid, Madrid, Spain
[10]Present address: Unidad de Presentación y Regulación Inmunes, Instituto de Salud Carlos III, Madrid, Spain
[11]Lead contact
*Correspondence: aramiro@cnic.es
https://doi.org/10.1016/j.celrep.2022.111468

SUMMARY

Atherosclerosis is a chronic inflammatory disease of the arteries that can lead to thrombosis, infarction, and stroke and is the leading cause of mortality worldwide. Immunization of pro-atherogenic mice with malondialdehyde-modified low-density lipoprotein (MDA-LDL) neo-antigen is athero-protective. However, the immune response to MDA-LDL and the mechanisms responsible for this athero-protection are not completely understood. Here, we find that immunization of mice with MDA-LDL elicits memory B cells, plasma cells, and switched anti-MDA-LDL antibodies as well as clonal expansion and affinity maturation, indicating that MDA-LDL triggers a bona fide germinal center antibody response. Further, *Prdm1*$^{fl/fl}$ *Aicda*-Cre$^{+/ki}$ *Ldlr*$^{-/-}$ pro-atherogenic chimeras, which lack germinal center-derived plasma cells, show accelerated atherosclerosis. Finally, we show that MDA-LDL immunization is not athero-protective in mice lacking germinal-center-derived plasma cells. Our findings give further support to the development of MDA-LDL-based vaccines for the prevention or treatment of atherosclerosis.

INTRODUCTION

Cardiovascular disease (CVD) remains the leading cause of mortality in the world, with most CVD deaths resulting from myocardial infarction and stroke. The main cause underlying thrombosis and CV events is atherosclerosis, a chronic disorder of large arteries caused by hyperlipidemia that leads to atheroma plaque formation (Hansson and Hermansson, 2011; Hansson et al., 2006; Lahoute et al., 2011; Libby, 2021; Skalen et al., 2002). Thus, there is a critical need to expand and improve our therapeutic and prognostic avenues to atherosclerosis (Libby, 2021; Nilsson and Hansson, 2020).

Atherosclerosis initiates with the infiltration and retention of cholesterol-rich low-density lipoprotein (LDL) particles in the subendothelial space of the artery wall (Skalen et al., 2002; Tabas et al., 2007). Retained LDL is subject to oxidation, which leads to diverse oxidized forms of LDL (OxLDL), including malondialdehyde-modified LDL (MDA-LDL) (Hansson and Hermansson, 2011; Lusis, 2000). OxLDL particles activate endothelial cells and induce the expression of adhesion molecules and chemokines that recruit monocytes to the intima layer and promote their differentiation into macrophages. At the intima, macrophages internalize OxLDL and eventually give rise to lipid-laden foam cells, which contribute to plaque growth and the generation of a necrotic core (Bobryshev et al., 2016; Brophy et al., 2017; Libby, 2021).

Adaptive immunity contributes in various and intertwined ways to atherosclerosis modulation. Different subsets of T cells have been ascribed different roles in atherosclerosis, which generally seem to stem from their pro- or anti-inflammatory properties (Ait-Oufella et al., 2006; Clement et al., 2015; Gupta et al., 1997; Nus et al., 2017; Saigusa et al., 2020). In the case of B cells, detailed studies on the contribution of different B cell subsets to atherosclerosis have revealed a complex landscape. B1 cells, a minor subset of B cells of fetal origin that produce natural immunoglobulin M (IgM) antibodies, are generally believed to be athero-protective (Kyaw et al., 2011; Rosenfeld et al., 2015; Shaw et al., 2000). Marginal zone B cells are splenic non-circulating B cells

that mediate an innate-like rapid antibody response to blood-borne antigens and have athero-protective capabilities (Nus et al., 2017). Follicular B cells are essential for long-lasting, T-dependent antibody responses and have been assigned both pro-atherogenic and athero-protective roles (Ait-Oufella et al., 2010; Caligiuri et al., 2002; Grasset et al., 2015; Kyaw et al., 2010, 2013; Major et al., 2002; Sage et al., 2012).

Upon antigen encounter and in the presence of T cell help, follicular B cells became activated and can engage into the germinal center (GC) reaction and give rise to long-lived memory B cells (MBCs) and high-affinity plasma cells (PCs) with alternate isotypes. Key to these antibody responses are the class switch recombination (CSR) and the somatic hypermutation (SHM) reactions. CSR is a recombination reaction that exchanges the primary IgM constant region by a downstream constant region, generating IgG, IgA, or IgE isotypes. SHM introduces changes in the antigen-recognizing, variable region of antibody genes thus giving rise to clonal variants. Coupled to affinity maturation, SHM allows the generation of higher affinity antibodies. Thus, GCs are essential for high-affinity humoral responses and underlie the protective mechanism of many vaccination strategies. Disruption of T-B cell interactions, abrogation of the GC reaction, or broad depletion of PCs resulted in smaller plaques (Tay et al., 2018), but they showed more instability (Centa et al., 2019). On the other hand, pro-atherogenic mice where antibody secretion was abolished had larger plaques (Sage et al., 2017). These results reveal a complex role of the antibody response in atherosclerosis. Of note, the role of antibody responses after specific challenge with atherosclerosis antigens was not addressed in these studies.

Indeed, very few antigens have been associated with atherosclerosis. The atherosclerosis adaptive immune response is thought to be triggered by self- and neo-antigens generated during disease development, the paradigm of which are oxidation-specific epitopes present in OxLDL (Nilsson and Hansson, 2020). Heat shock protein (Hsp) 60, a mitochondrial chaperone, has also been associated with atherosclerosis (Almanzar et al., 2012; George et al., 1999; Xu et al., 1992, 1993; Zhu et al., 2001). In addition, the aldehyde dehydrogenase 4 family member A1 (ALDH4A1) mitochondrial protein has been recently identified as an auto-antigen in atherosclerosis (Lorenzo et al., 2021). Circulating ALDH4A1 is increased in mice and humans with atherosclerosis, and anti-ALDH4A1 antibody is athero-protective (Lorenzo et al., 2021). However, LDL forms have been by far the most studied atherosclerosis antigen and, as of today, are considered the best antigenic target for the design of atherosclerosis vaccines (Nilsson and Hansson, 2020). T cells, B cells, and anti-OxLDL antibodies have been found in atheroma plaques and in plasma from atherogenic mice, rabbits, and humans (Hansson et al., 1989; Hollander et al., 1979; Jonasson et al., 1986; Karvonen et al., 2003; Palinski et al., 1989, 1994; Tsimikas et al., 2007).

MDA forms covalent adducts with lysine residues of the apoB-100 protein and generates MDA-LDL, the predominant form of OxLDL (Hartley et al., 2019; Yla-Herttuala et al., 1989). MDA-LDL immunization reduces atherosclerosis (Fredrikson et al., 2003; George et al., 1998; Palinski et al., 1995; Zeng et al., 2018; Zhou et al., 2001), but the immune response to MDA-LDL is not completely understood, and several mechanisms have been proposed to explain MDA-LDL-mediated athero-protection (Ait-Oufella et al., 2006; Binder et al., 2004; Hjerpe et al., 2010; Zhou et al., 2005).

Here, we find that athero-protective MDA-LDL immunization triggers an antibody immune response that entails GC formation and the generation of MBCs and PCs. A high-throughput single-cell analysis of the immunoglobulin repertoire in MDA-LDL-immunized mice revealed clonal expansion and accumulation of SHM, featuring a GC response. Using *Prdm1*$^{fl/fl}$ *Aicda*-Cre$^{+/ki}$ *Ldlr*$^{-/-}$ chimeras, we further show that depletion of GC-derived PCs aggravates atherosclerosis, indicating a global athero-protective role of these cells. Finally, we found that athero-protection by MDA-LDL immunization is impaired in *Prdm1*$^{fl/fl}$ *Aicda*-Cre$^{+/ki}$ *Ldlr*$^{-/-}$ chimeras. Together, our results indicate that MDA-LDL immunization triggers a bona fide GC reaction and the generation of GC-derived PCs, which contribute to athero-protection.

RESULTS

Athero-protective MDA-LDL immunization induces GC reactions

To gain insights into the impact of MDA-LDL immunization on atherosclerosis, we immunized *Ldlr*$^{-/-}$ mice with MDA-LDL in complete Freund's adjuvant (CFA) or with CFA alone as described before (Figure 1A) (Freigang et al., 1998). We did not detect significant differences in weight gain or plasma lipids between groups (Figure S1A; Table S1). Quantification of atherosclerotic plaques in aortic roots showed a significant decrease in atherosclerosis extension in mice immunized with MDA-LDL + CFA compared with those immunized with CFA alone (Figures 1B–1D), as previously described (Freigang et al., 1998; George et al., 1998; Palinski et al., 1995; Turunen et al., 2015). We did not detect changes in the proportions of GC B cells or total PCs (Figures S1B–S1G). However, the proportion of MBCs was significantly increased in MDA-LDL + CFA-immunized mice compared with CFA controls (Figure 1E). Likewise, the proportion of IgG1$^+$ PCs was much larger in MDA-LDL + CFA mice (Figure 1F). Indeed, IgM, IgG1, IgG2b, and IgG2c MDA-LDL-specific antibodies were greatly increased in serum from MDA-LDL-immunized mice (Figure 1G). Thus, MDA-LDL immunization of *Ldlr*$^{-/-}$ mice is athero-protective and promotes a B cell response that generates MBCs, switched PCs, and MDA-LDL-specific switched antibodies.

To dissect the B cell immune response to MDA-LDL in the absence of atherosclerosis-dependent variables, we performed immunization experiments in *Aicda*-Cre$^{+/ki}$ (Robbiani et al., 2008; Rommel et al., 2013) *R26tdTom*$^{+/ki}$ mice (Madisen et al., 2010), where B cells that have been activated for activation-induced deaminase (AID) expression become irreversibly tdTom$^+$ (Figure S2). AID is the enzyme that initiates SHM and CSR; thus, its expression is a good proxy to identify cells that have had GC experience (Albright et al., 2019; Centa et al., 2019; Gitlin et al., 2016; Mayer et al., 2020). *Aicda*-Cre$^{+/ki}$ *R26tdTom*$^{+/ki}$ mice were immunized with MDA-LDL + CFA or with CFA alone as shown in Figure 2A. We detected an increase in tdTom$^+$GL7$^+$ GC B cells and tdTom$^+$PDL-2$^+$ MBCs in lymph nodes and spleen of MDA-LDL + CFA-immunized mice (Figures 2B–2D; GC absolute numbers

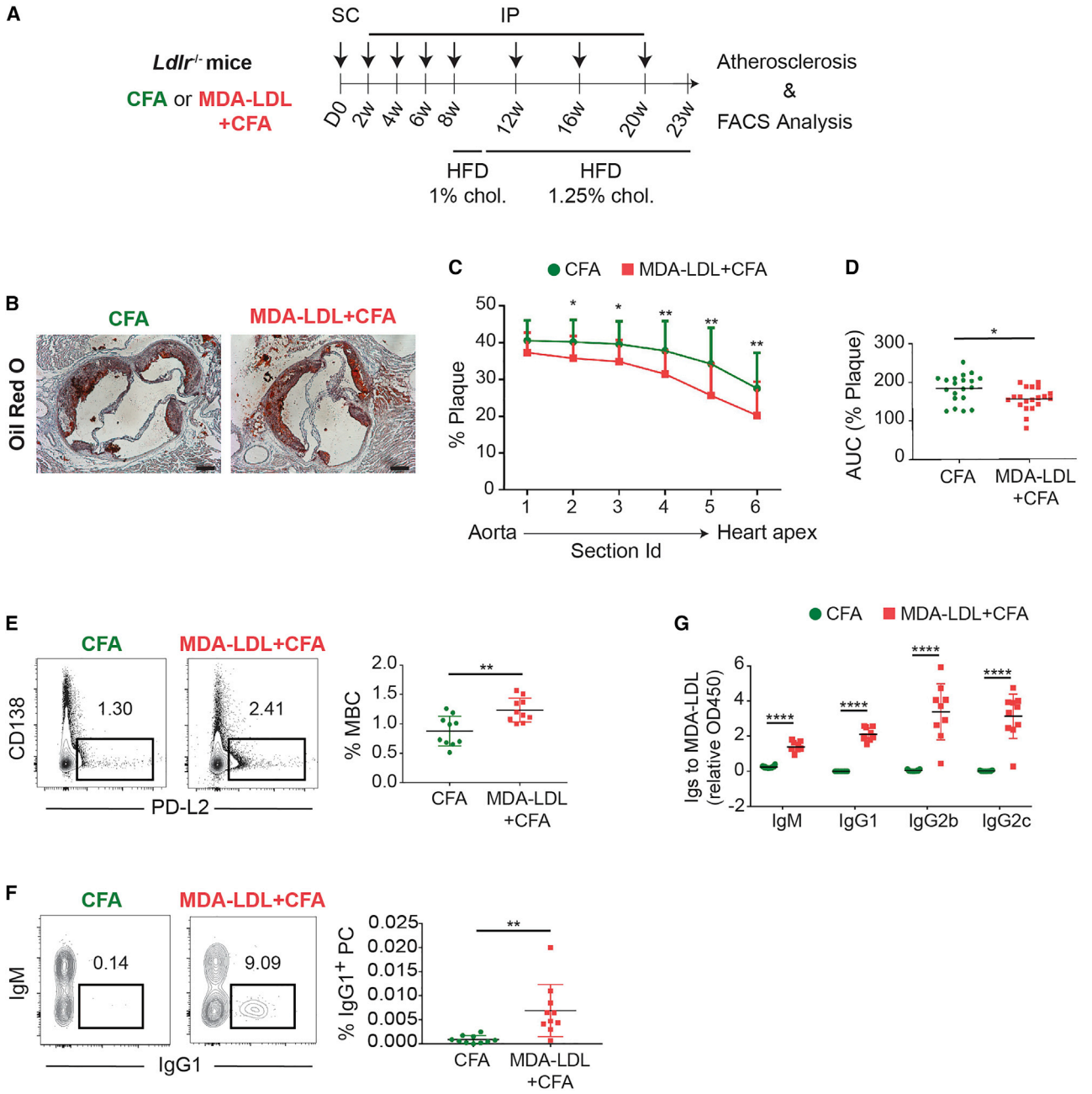

Figure 1. MDA-LDL is athero-protective and promotes a specific humoral response

(A) Experimental design. *Ldlr*$^{-/-}$ mice were immunized subcutaneously (s.c.) with MDA-LDL in CFA or with CFA alone (day 0). Four booster immunizations were done given intraperitoneally (i.p.) with MDA-LDL in IFA or IFA alone every two weeks (weeks 2, 4, 6, 8), followed by three additional immunizations once a month four weeks later (week 12, 16, 20). Mice were fed with 1% cholesterol HFD and with 1.25% cholesterol HFD from weeks 8–10 and 10–23, respectively.

(B) Representative Oil red O/Hematoxylin staining and (C) quantification of the proportion of atheroma plaque in serial 80 μm-spaced aortic sinus cryosections from MDA-LDL + CFA and CFA immunized mice.

(D) Area under the curve (AUC) plot of atheroma plaque quantification. The scale bars in images represents 200 μm. Representative flow cytometry plots and quantification of (E) splenic MBCs (B220^{+}PD-L2^{+}) and (F) IgG1^{+} bone marrow PCs (B220^{-}CD138^{+}IgG1^{+}) from MDA-LDL + CFA and CFA mice. Population percentages in FACS graphs indicate the frequency of live cells.

(G) Quantification by ELISA of MDA-LDL specific IgM, IgG1, IgG2b and IgG2c levels in serum from LDLR$^{-/-}$ mice 23 weeks after primary immunization with MDA-LDL + CFA or CFA. Data analyzed by unpaired t and two-way ANOVA statistical tests. All experiments were performed with 21–28-week-old males. Each dot in the graphs represents a biological replicate (individual mouse). *$p \leq 0.05$, **$p < 0.01$ and ****$p < 0.0001$.

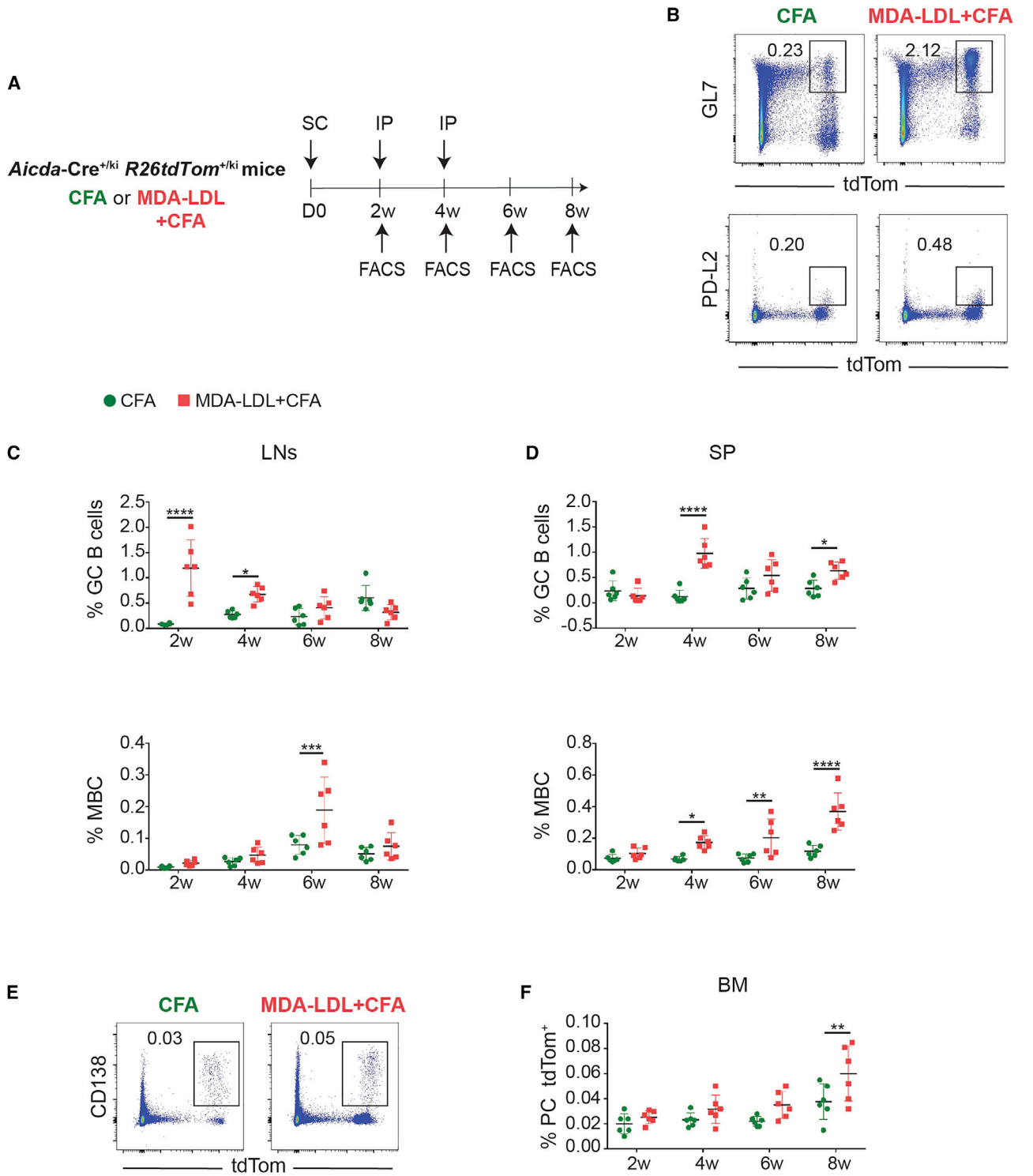

Figure 2. MDA-LDL immunization triggers a GC B cell response in non-atherogenic mice

(A) Experimental design. Mice were immunized SC with MDA-LDL in CFA or with CFA alone, followed by two booster immunizations IP with MDA-LDL in incomplete FA (IFA) or IFA alone 2 and 4 weeks later. Fluorescence-activated cell sorting (FACS) analyses were performed 2, 4, 6, and 8 weeks after the primary immunization.

(B–D) Representative FACS plots of GC B cells ($B220^+GL7^+tdTom^+$; top panel) and MBCs ($B220^+PD\text{-}L2^+tdTom^+$; bottom panel) 2 and 6 weeks after primary immunization, respectively (B), and quantification of these populations in (C) lymph nodes (LNs) and (D) spleen (SP).

(legend continued on next page)

shown in Figures S2B and S2C). GC B cells were also detected in C57-BL6 mice after a single MDA-LDL immunization (Figure S2D). In addition, PCs accumulated over time in the bone marrow and were significantly increased 2 weeks after the third immunization (Figures 2E and 2F). This response was accompanied by an increase in both unswitched and switched anti-MDA-LDL antibody titers in MDA-LDL-immunized mice, as measured by enzyme-linked immunosorbent assay (ELISA) (Figures 3A–3D).

To further analyze the specificity of the antibody response to MDA-modified epitopes, we measured the antibody titers to BSA oxidized with MDA (MDA-BSA) in plasma from MDA-LDL + CFA-, CFA-, and PBS-immunized mice. We found that MDA-LDL immunization led to a dramatic increase in both IgM and IgG anti-MDA-BSA antibody titers (Figure 3E). In addition, competition immunoassays with plasma from MDA-LDL-immunized mice showed that binding of plasma IgG1 antibodies to MDA-LDL was partially inhibited by pre-incubation with MDA-BSA and LDL particles, while MDA-LDL completely inhibited the binding of antibodies to MDA-LDL, indicating high specificity of the anti-MDA-LDL; in this case, IgG1 switched antibodies (Figure 3F).

Together, these results indicate that MDA-LDL immunization triggers an immune GC response that gives rise to antibodies specific for MDA-containing epitopes.

SHM and selection in MDA-LDL-immunized mice

To gain molecular insights into the antibody response to MDA-LDL, we analyzed the immunoglobulin repertoire by single-cell sequencing of Ig genes in *Aicda*-Cre$^{+/ki}$ *R26tdTom*$^{+/ki}$ mice immunized with MDA-LDL in CFA or CFA alone. We performed single-cell sorting and sequencing of GC B cells (B220^{+} GL7^{+} tdTom^{+}) and MBCs (B220^{+} GL7^{-} tdTom^{+}) from lymph nodes and GC-derived PCs (B220^{-} CD138^{+} tdTom^{+}) from bone marrow (Figure 4A and S3A). We obtained 597 heavy chain (IgH) and light chain (IgL) paired sequences from three mice immunized with MDA-LDL and two mice immunized with CFA alone (Table S2; Figures 4B and S3B). We found minor differences in the variable (V) and joining (J) gene J usage between the MDA-LDL + CFA and CFA repertoires (Figures S4A–S4F), with the VH2 family being more represented in MDA-LDL + CFA mice, and no differences in CDR3 length (Figures S4G and S4H). Conversely, VH5 and VH10 families were under-represented in the MDA-LDL + CFA repertoire (Figure S4A)

Regarding SHM, we did not observe significant differences in the proportion of mutated Igs or in their overall mutation frequency between the CFA and MDA-LDL + CFA groups (Figures 4C and 4D). However, while GC, MBC, and PC subsets showed similar SHM frequencies in the CFA group, in MDA-LDL-immunized mice, Igs from GC B cells were the most mutated, followed by the Igs from PCs, and with Igs from MBCs harboring the fewest mutations (Figure 4E). Moreover, only IgG1^{+} cells, but no other isotypes, showed a significant increase of SHM in MDA-LDL-immunized mice compared with control mice (Figures 4F and S4A–S4M), and MDA-LDL + CFA-immunized mice had a larger proportion of GC IgG1^{+} cells (Figures S4N–S4P). Together, these data indicate that MDA-LDL immunization triggers an immune response that involves a GC reaction.

To focus on Igs relevant to the MDA-LDL response, we identified those expressed by clonally expanded B cells. Thus, we defined "B cell clones" as clusters of three or more Igs sharing the same V and J genes and the same CDR3 length in both IgH and IgL. We identified 25 B cell clones, 12 of which were exclusively comprised by Igs from the CFA group (1–12), 12 by Igs from the MDA-LDL + CFA group (13–24) (from now on, exclusive clones), and 1 clone containing Igs from both groups (25) (mixed clone) (Table S3; Figure 4G).

We found that exclusive CFA clones were disproportionally comprised by Igs expressed by GC B cells, while MDA-LDL + CFA clones were composed by Igs from GC, PC, and MBC populations (Figure 4H) and showed a greater enrichment in PCs (Figure 4I). Finally, while in CFA mice we did not observe differences in mutation frequency between expanded and non-expanded Igs, in MDA-LDL + CFA mice, expanded Igs had a higher mutational load than non-expanded Igs (Figure 4J). This result shows that B cells expanded in response to MDA-LDL express heavily mutated Igs, indicating that they have undergone affinity maturation.

GC-derived PCs are athero-protective

To address the role of GC-derived antibodies in atherosclerosis, we transferred bone marrow cells from *Prdm1*$^{fl/fl}$ *Aicda*-Cre$^{+/ki}$ CD45.2 mice into lethally irradiated *Ldlr*$^{-/-}$ mice expressing the CD45.1 allotype (from now on, *Prdm1*$^{fl/fl}$ *Aicda*-Cre$^{+/ki}$ *Ldlr*$^{-/-}$ chimeras). *Prdm1* codes for Blimp1, the master transcriptional regulator of PCs (Shaffer et al., 2002); thus, *Prdm1*$^{fl/fl}$ *Aicda*-Cre$^{+/ki}$ *Ldlr*$^{-/-}$ chimeras will be devoid of PCs and antibody secretion derived of cells that have expressed AID. *Ldlr*$^{-/-}$ CD45.1^{+} mice transferred with CD45.2^{+} *Prdm1*$^{+/+}$ *Aicda*-Cre$^{+/ki}$ bone marrow (from now on, *Prdm1*$^{+/+}$ *Aicda*-Cre$^{+/ki}$ *Ldlr*$^{-/-}$ chimeras) were used as controls (Figure 5A). *Prdm1*$^{+/+}$ *Aicda*-Cre$^{+/ki}$ *Ldlr*$^{-/-}$ and *Prdm1*$^{fl/fl}$ *Aicda*-Cre$^{+/ki}$ *Ldlr*$^{-/-}$ chimeras had comparable proportions of CD45.2+ donor-derived cells and of residual CD45.1^{+} host-derived cells (Figures S5A and S5B). Following bone marrow reconstitution, chimeras were fed with a high-fat diet (HFD) for 9 weeks. We found no significant differences in weight gain (Figure S5C) or plasma lipid profile (Table S4) between the two groups.

Expectedly, the proportion of CD138^{+} PCs was reduced in the spleens of *Prdm1*$^{fl/fl}$ *Aicda*-Cre$^{+/ki}$ *Ldlr*$^{-/-}$ chimeras compared with control mice (Figure 5B). This reduction was more severe in IgG2b isotype-switched PCs (Figure 5C), suggesting that the CD138^{+}IgM^{+} PCs remaining in *Prdm1*$^{fl/fl}$ *Aicda*-Cre$^{+/ki}$ *Ldlr*$^{-/-}$ chimeras probably represent PCs derived from extrafollicular B cells. Likewise, plasma IgM and IgG antibody titers were reduced in *Prdm1*-deficient chimeras (Figures 5D and 5E). These

(E and F) Representative FACS plots of bone marrow (BM) tdTom^{+} PCs (B220^{-}CD138^{+}tdTom^{+}) 4 weeks after the primary immunization (E) and quantification (F). GC and MBC FACS analysis was performed on 6- to 8-week-old male (n = 27) and female (n = 21) mice. PC FACS analysis was performed on 6- to 8-week-old male (n = 16) and female (n = 8) mice.

Each dot in the graphs represents a biological replicate (individual mouse). Population percentages in FACS graphs indicate the frequency of live cells. Data analyzed by two-way ANOVA statistical test. *p $\leq$ 0.05, **p < 0.01, ***p < 0.001, and ****p < 0.0001.

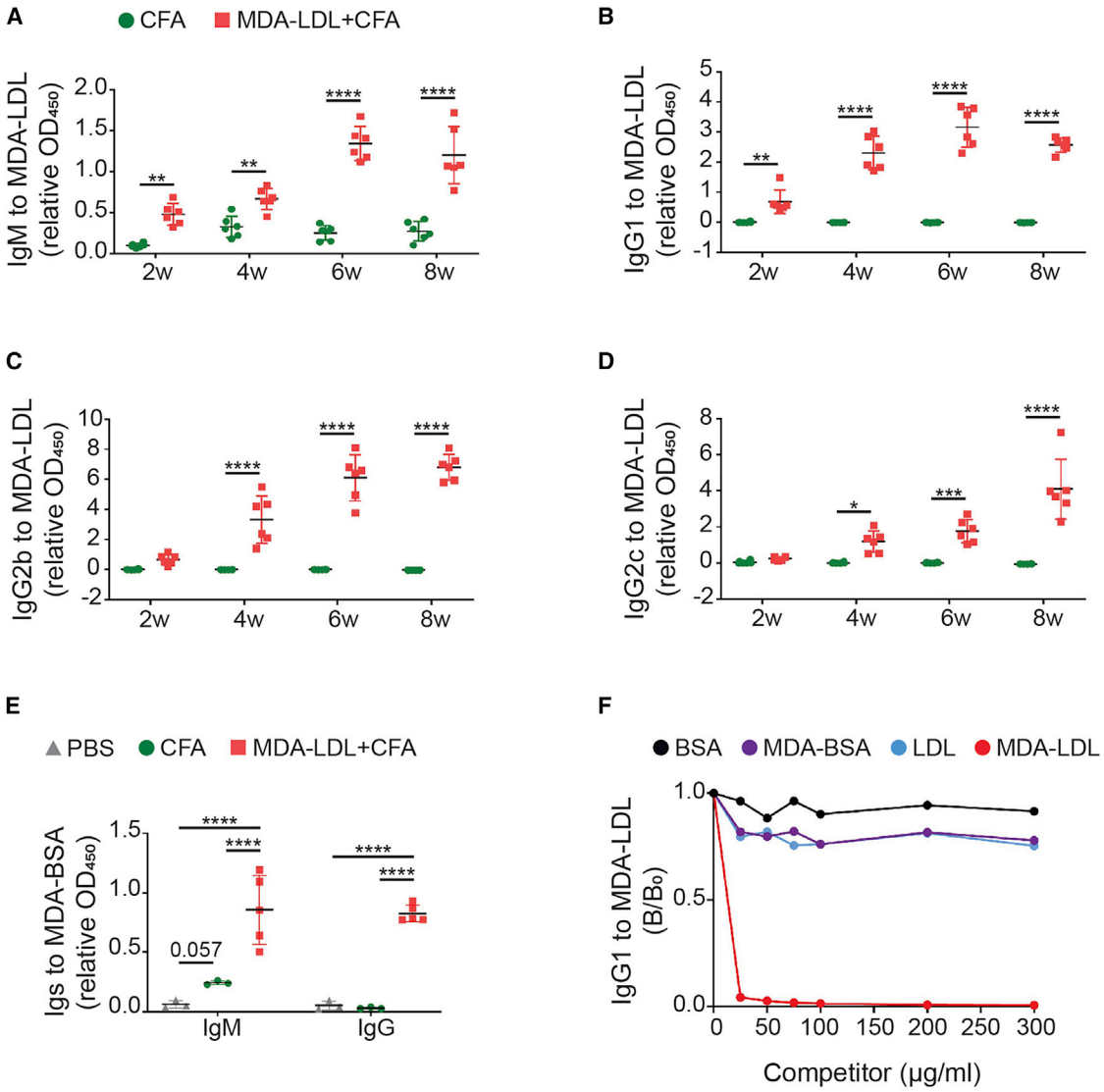

Figure 3. Anti-MDA-LDL antibodies recognize epitopes only presented in the MDA-modified LDL

Plasma antibody levels in *Aicda*-Cre$^{+/ki}$ *R26tdTom*$^{+/ki}$ mice immunized with CFA alone or MDA-LDL + CFA as determined by ELISA.

(A–D) Quantification of (A) IgM, (B) IgG1, (C) IgG2b, and (D) IgG2c anti-MDA-LDL antibodies 2, 4, 6, and 8 weeks after primary immunization.

(E) Quantification of IgM and IgG anti-MDA-BSA antibodies 6 weeks after primary immunization.

(F) Competition immunoassay to measure anti-MDA-LDL IgG1 antibodies. Plasma IgG1 binding to plated MDA-LDL was quantified in the presence (B) or absence (B_0) of increasing concentrations (0, 25, 50, 100, 150, 200, and 300 μg/mL) of the indicated competitors (BSA, MDA-BSA, LDL, and MDA-LDL). Results are expressed as ratios of IgG1 binding to MDA-LDL in the presence (B) or absence (B_0) of the competitor.

Each dot in the graphs represents a biological replicate (individual mouse). Data analyzed by one-way and two-way ANOVA statistical tests. *$p \leq 0.05$, **$p < 0.01$, ***$p < 0.001$, and ****$p < 0.0001$.

results indicate that a large proportion of PCs, including those derived from GC B cells, are depleted in our *Prdm1*$^{fl/fl}$ *Aicda*-Cre$^{+/ki}$ *Ldlr*$^{-/-}$ model.

To assess the contribution of GC-derived PC on atherosclerosis, we evaluated atherosclerosis progression in *Prdm1*$^{fl/fl}$ *Aicda*-Cre$^{+/ki}$ *Ldlr*$^{-/-}$ and *Prdm1*$^{+/+}$ *Aicda*-Cre$^{+/ki}$ *Ldlr*$^{-/-}$ chimeras. Atherosclerosis quantification in aortic sinus revealed a significant increase in atherosclerosis in *Prdm1*-deficient chimeras compared with in controls (Figures 5F–5H). Atherosclerosis acceleration did not associate with obvious differences in atheroma plaque composition and stability as measured by staining of collagen content and necrotic core analysis (Figures S5D–S5G), as well as macrophage and smooth muscle cell (SMC) immunofluorescence (Figures S5H–S5J). We conclude that GC-derived PCs and/or antibodies protect from atherosclerosis development.

GC-derived antibodies contribute to MDA-LDL immunization-mediated athero-protection

To assess the role of GC-derived antibodies in MDA-LDL-mediated athero-protection, we immunized *Prdm1*-deficient

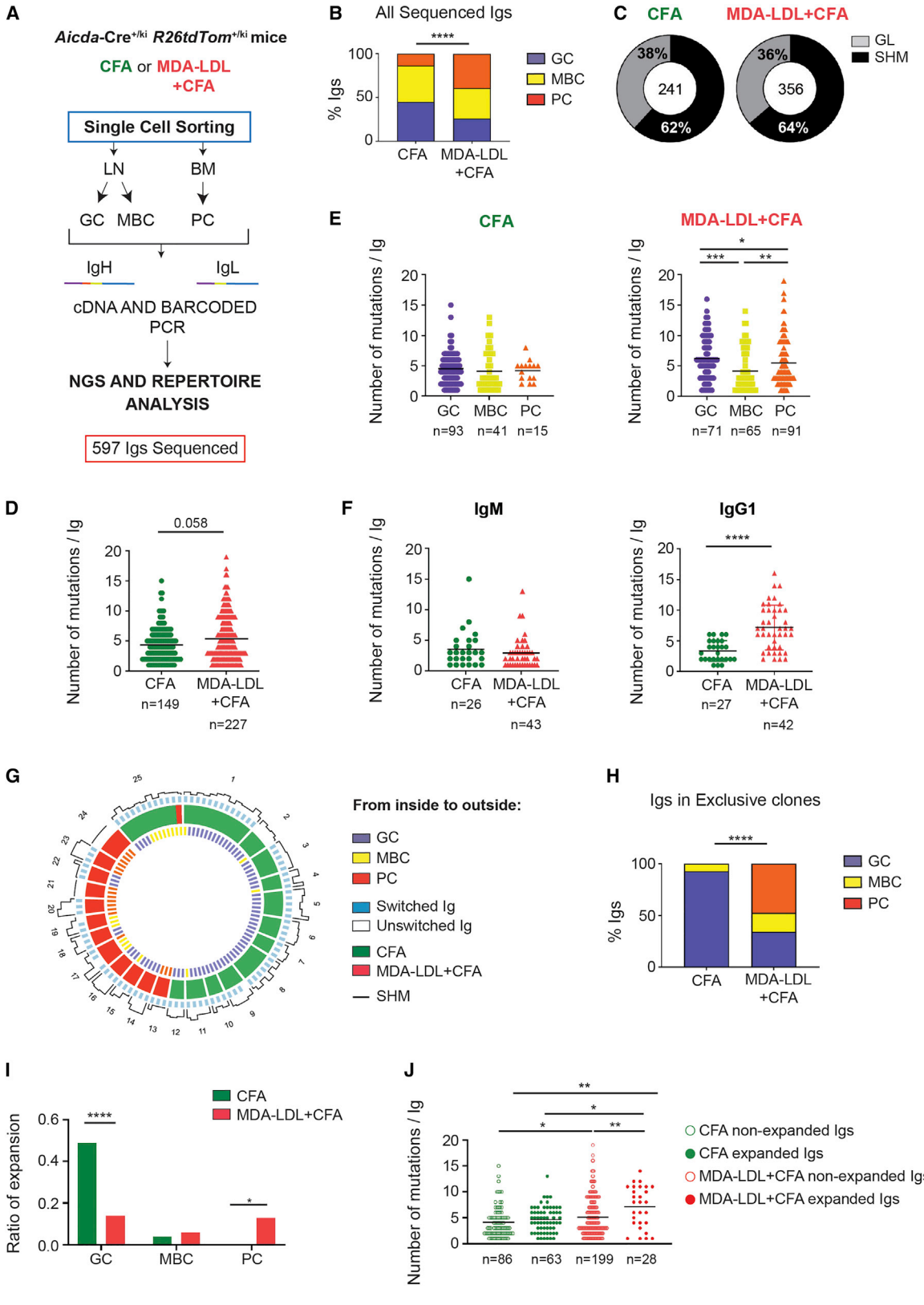

(legend on next page)

pro-atherogenic chimeras with MDA-LDL. Briefly, we transferred bone marrow from *Prdm1*$^{fl/fl}$ *Aicda*-Cre$^{+/ki}$ or *Prdm1*$^{+/+}$ *Aicda*-Cre$^{+/ki}$ CD45.2 mice into *Ldlr*$^{-/-}$ CD45.1 mice, and reconstituted chimeras were immunized with MDA-LDL + CFA, CFA, or PBS and fed with an HFD as indicated in Figure 6A. Chimeras from all 6 groups showed similar weight gain (Figure S6). Plasma levels of total cholesterol, free cholesterol, LDL cholesterol, and triglyceride pro-atherogenic indexes (Talayero and Sacks, 2011), but not high-density lipoprotein (HDL) cholesterol, tended to be reduced in CFA- and MDA-LDL + CFA-immunized chimeras (Figure S7). Reduction in pro-atherogenic lipid levels was observed both in *Prdm1*-proficient and -deficient chimeras, indicating that modulation of the plasma lipid profile seems to be independent of GC-derived antibodies (Abs).

Expectedly, we found that the PC population was reduced in the spleen of MDA-LDL + CFA-immunized *Prdm1*$^{fl/fl}$ *Aicda*-Cre$^{+/ki}$ *Ldlr*$^{-/-}$ compared with immunized control chimeras (Figure 6B). Plasma titers of IgG Abs were also reduced in MDA-LDL-immunized *Prdm1*$^{fl/fl}$ *Aicda*-Cre$^{+/ki}$ *Ldlr*$^{-/-}$ chimeras (Figure 6C), while total IgM titers were not significantly changed (Figure 6D). Likewise, *Prdm1*-deficient pro-atherogenic chimeras showed a sharp decrease in anti-MDA-LDL IgG1, IgG2b, and IgG2c Ab titers (Figures 6E–6G) and a mild reduction of anti-MDA-LDL IgM Ab titers (Figure 6H). These results indicate that PCs derived from GCs play a critical role in the Ab response triggered by MDA-LDL immunization in atherosclerotic mice.

To test the role of GC-derived Abs in atherosclerosis, we then measured atherosclerotic extent in aortic sinus of *Prdm1*$^{+/+}$ *Aicda*-Cre$^{+/ki}$ *Ldlr*$^{-/-}$ and *Prdm1*$^{fl/fl}$ *Aicda*-Cre$^{+/ki}$ *Ldlr*$^{-/-}$ chimeras immunized with MDA-LDL in CFA or CFA alone (experiment depicted in Figure 6A; Figures 7A and 7B). We found that both *Prdm1*$^{+/+}$ *Aicda*-Cre$^{+/ki}$ *Ldlr*$^{-/-}$ and *Prdm1*$^{fl/fl}$ *Aicda*-Cre$^{+/ki}$ *Ldlr*$^{-/-}$ chimeras treated with CFA developed atherosclerotic plaques of similar size (Figure 7C), indicating that CFA athero-protection is independent of GC-derived Abs. In contrast, upon MDA-LDL immunization, *Prdm1*$^{fl/fl}$ *Aicda*-Cre$^{+/ki}$ *Ldlr*$^{-/-}$ chimeras had larger aortic plaque lesions than did *Prdm1*-proficient chimeras (Figure 7D). Therefore, these results indicate that PCs and Abs derived from GC-experienced B cells drive MDA-LDL-mediated athero-protection.

DISCUSSION

Here, we have shown that MDA-LDL immunization of proatherogenic *Ldlr*$^{-/-}$ mice triggers an Ab immune response that entails the generation of GCs, switched Abs, MBCs, and PCs. Our experiments in *Aicda*-Cre$^{+/ki}$ *R26tdTom*$^{+/ki}$ mice have allowed us to trace activated B cells after MDA-LDL immunization and have confirmed this GC response in a non-atherogenic background, thus eliminating the confounding effects that the atherosclerosis immune response might have. Interestingly, we detected Abs specific of the MDA moiety in the context of the LDL particle. Thus, although native LDL by itself can raise an immune response (Gistera et al., 2018), our data support that MDA-modified LDL is indeed immunogenic, in agreement with previous data (Freigang et al., 1998). Of note, our results were obtained by comparing MDA-LDL in CFA with mice immunized with CFA alone, which is also known to promote athero-protection (Hansen et al., 2001). Interestingly, MDA-LDL promotes an increase in the load of SHM, particularly in expanded clones of B cells, strongly suggesting that affinity maturation is in place in MDA-LDL-immunized mice, and, therefore, that MDA-LDL, but not CFA alone, triggers a bona fide GC response, much like other antigenic triggers used for vaccination strategies (Gómez-Escolar et al., 2021; Weisel et al., 2016). In this regard, it is worth mentioning that the Goal of Oxidized LDL and Activated Macrophage Inhibition by Exposure to a Recombinant Antibody (GLACIER) trial was approved to assess the athero-protective properties of passive immunization with the monoclonal anti-MDA MLDL1278A Ab. The results did not reveal athero-protective effects, at least in the cohort of subjects with stable CVD analyzed in the trial (Lehrer-Graiwer et al., 2015; Nilsson and Hansson, 2020). However, it is tempting to suggest that alternative Abs can prove valuable candidates in future clinical trials. Therefore, evaluation of athero-protection after passive transfer of Abs from expanded clones identified in our study, either individually or in combination, can provide proof of concept for such strategies.

In our study, we have addressed the general contribution of GC-derived Abs using *Prdm1*$^{fl/fl}$ *Aicda*-Cre$^{+/ki}$ mice. In this model, cells that have activated AID expression are depleted of *Prdm1*. We found that *Prdm1*$^{fl/fl}$ *Aicda*-Cre$^{+/ki}$ *Ldlr*$^{-/-}$ chimeras showed increased atherosclerosis, indicating an athero-protective effect

Figure 4. Single-cell antibody sequencing from single cells of MDA-LDL-immunized mice

(A) GC B cells and MBCs from LNs and GC-derived PCs (PC tdTom+) from BM of CFA- (n = 2) and MDA-LDL + CFA-immunized (n = 3) mice (3 times every 2 weeks) were isolated 2 weeks after last boost by flow cytometric single-cell sorting. IgH and IgL genes were amplified and sequenced. Paired *Igh* and *Igk*/*Igl* gene sequences from a total of 597 Igs were obtained and analyzed.

(B) Population distribution of all Igs sequenced within each group.

(C) Proportion of mutated (SHM) and germ line (GL) Igs in CFA and MDA-LDL + CFA repertoires.

(D–F) Number of IgH somatic mutations (nucleotide exchanges) within mutated Igs in (D) all cells, (E) by cell population, and (F) in IgM and IgG1 B cells from each group.

(G) Circos plots illustrate the molecular features of expanded Igs. Igs from clonally expanded cell clones are represented as boxes filled in green (CFA exclusive clones), red (MDA-LDL + CFA exclusive clones), and both colors (shared clones). Clone number is shown in the outer layer. Cell population origin, CSR, and number of Ig mutations (SHM) (nucleotide exchanges) are indicated for each B cell.

(H) Population distribution of Igs present in exclusive clones from each group.

(I) Ratio of expansion (expanded cells/all cells) of each cell population.

(J) Number of somatic mutations (nucleotide exchanges) per mutated non-expanded Ig or expanded Ig in each group. Single-cell antibody sequencing experiment was performed using samples from 2 and 3 mice immunized with CFA or MDA-LDL + CFA, respectively.

Data analyzed by non-parametric Mann-Whitney statistical test and chi-square test (A–F) and by non-parametric Kruskal-Wallis statistical, Fisher's exact, and chi-square tests (G–J). *p $\leq$ 0.05, **p < 0.01, ***p < 0.001, and ****p < 0.0001.

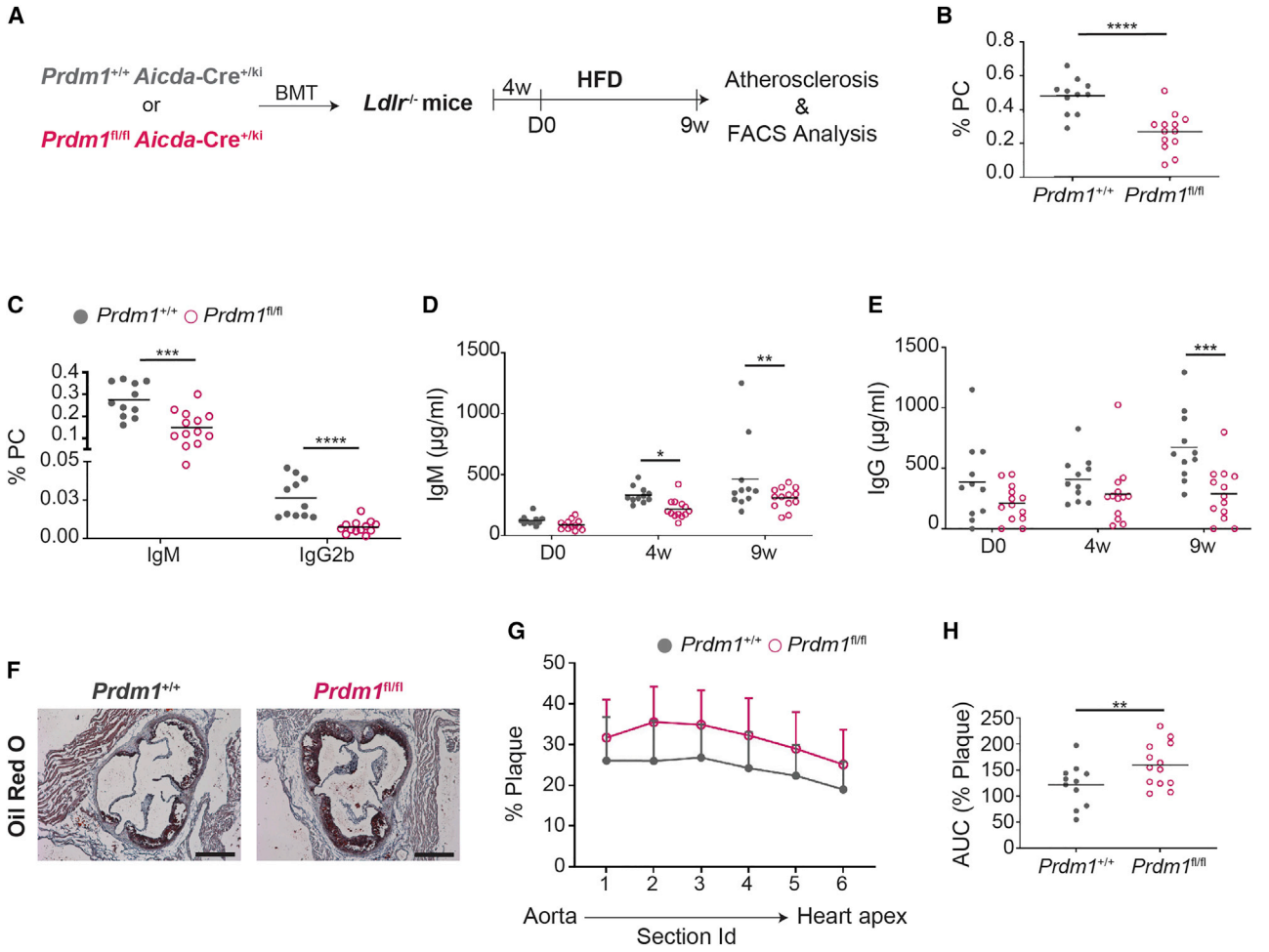

Figure 5. *Prdm1*$^{fl/fl}$ *Aicda*-Cre$^{+/ki}$ *Ldlr*$^{-/-}$ chimeras show increased atherosclerosis

(A) Experimental design. BM from *Prdm1*$^{+/+}$ *Aicda*-Cre$^{+/ki}$ or *Prdm1*$^{fl/fl}$ *Aicda*-Cre$^{+/ki}$ mice was isolated and intravenously (i.v.) transferred to previously irradiated *Ldlr*$^{-/-}$ mice. Four weeks after BM transfer, mice were fed with a 0.2% cholesterol HFD for 9 weeks.

(B and C) Quantification of (B) PC percentage (B220$^{-/low}$CD138^{+}) and (C) IgM-positive (B220$^{-/low}$CD138^{+}IgM^{+}) and IgG2b-positive (B220$^{-/low}$CD138^{+}IgG2b^{+}) PCs in SP.

(D and E) Quantification of total (D) IgM and (E) IgG antibody titers in plasma at day 0 and after 4 and 9 weeks of HFD as measured by ELISA.

(F and G) Representative oil red O/hematoxylin stains (F) and quantification (G) of the proportion of atheroma plaque in serial 80 μm-spaced aortic sinus cryosections from *Prdm1*$^{+/+}$ and *Prdm1*$^{fl/fl}$ *Aicda*-Cre$^{+/ki}$ *Ldlr*$^{-/-}$ chimeras.

(H) Area under the curve (AUC) plot of atherosclerosis quantification. The scale bars in images represent 200 μm. The experiment was performed with 18 male and 6 female 11-week-old receptors.

Each dot in the graphs represents a biological replicate (individual mouse). Data analyzed by unpaired t statistical test and two-way ANOVA statistical test. *p ≤ 0.05, **p < 0.01, ***p < 0.001, and ****p < 0.0001.

of GC-derived PCs and/or Abs. Two *Prdm1* models have been previously reported in the context of atherosclerosis with diverse results, which may be explained by the different experimental strategies for *Prdm1* deletion. In one study, *Prdm1* deletion was driven by a *Cd23*-Cre, thus driving effective depletion of Blimp1 from all follicular-derived B cells (Tay et al., 2018). In a second study, *Prdm1* deletion was driven by the *Cd19*-Cre allele, leading to Blimp1 deletion in the vast majority of B cells (Centa et al., 2019). Although the onset of AID expression shortly precedes B cell entry into the GC, our approach allows a more restricted depletion of GC-derived PCs than previous reports. This is further indicated by the persistence of a considerable fraction of IgM^{+} PCs in *Prdm1*$^{fl/fl}$ *Aicda*-Cre$^{+/ki}$ mice. Therefore, it is possible that Ab-secreting cells depleted in the *Cd19*-Cre or *Cd23*-Cre models—but not in *Prdm1*$^{fl/fl}$ *Aicda*-Cre$^{+/ki}$ mice—have pro-atherogenic properties. Interestingly, abolishing Ab secretion by deletion of *Xbp-1* with *mb1*-Cre, which is expressed from early B cell precursors, resulted in increased atherosclerosis, as did depletion of T cells with anti-CD4 Abs (Sage et al., 2017). These results suggest that the endogenous T cell-dependent response can be athero-protective (Sage et al., 2017), in agreement with our results. In addition, the differential impact on atherosclerosis observed in these models may be the consequence of a subtle functional balance between Abs with different antigen

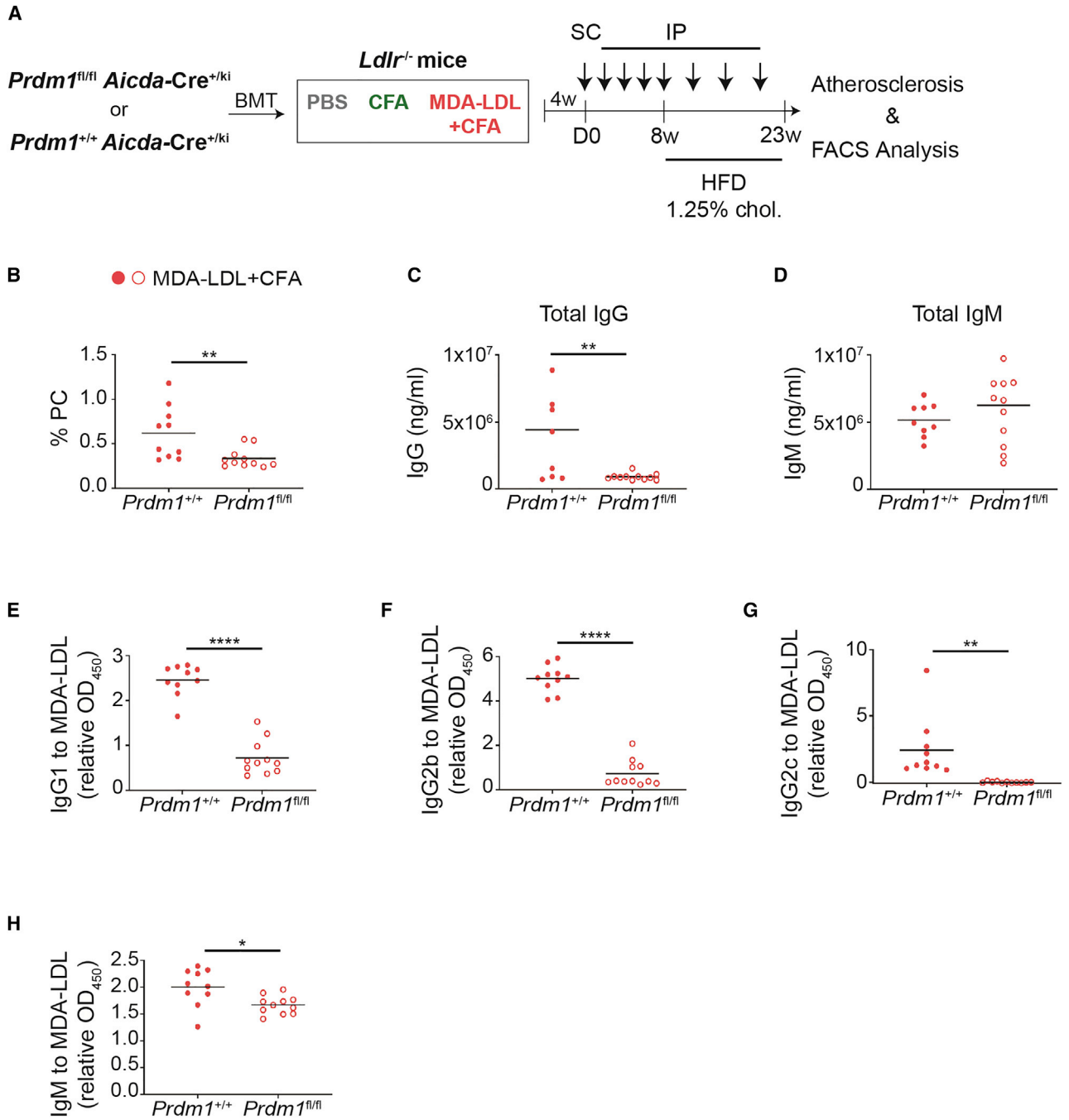

Figure 6. Low MDA-LDL-specific antibody responses in the absence of GC-derived PCs

(A) Experimental design. BM from *Prdm1*$^{+/+}$ *Aicda*-Cre$^{+/ki}$ or *Prdm1*$^{fl/fl}$ *Aicda*-Cre$^{+/ki}$ mice was i.v. transferred to into irradiated *Ldlr*$^{-/-}$ recipients. Four weeks later, mice were immunized with MDA-LDL + CFA, CFA alone, or PBS and fed an HFD with 1.25% cholesterol for 15 weeks. Twenty-three weeks after the primary immunization, mice were sacrificed for analysis.

(B) Quantification of SP PCs (B220$^{-/low}$CD138^{+}) from MDA-LDL + CFA-immunized *Prdm1*$^{+/+}$ and *Prdm1*$^{fl/fl}$ *Aicda*-Cre$^{+/ki}$ *Ldlr*$^{-/-}$ chimeras by FACS.

(C and D) ELISA-based quantification of total (C) IgG and (D) IgM antibody levels in plasma from *Prdm1*$^{+/+}$ and *Prdm1*$^{fl/fl}$ *Aicda*-Cre$^{+/ki}$ *Ldlr*$^{-/-}$ chimeras immunized with MDA-LDL + CFA.

(E–H) MDA-LDL-specific (E) IgG1, (F) IgG2b, (G) IgG2c, and (H) IgM antibody levels in *Prdm1*$^{+/+}$ and *Prdm1*$^{fl/fl}$ *Aicda*-Cre$^{+/ki}$ *Ldlr*$^{-/-}$ chimeras immunized with MDA-LDL + CFA measured by ELISA. All experiments were performed with 8- to 9-week-old male receptors.

Each dot in the graphs represents a biological replicate (individual mouse). Data analyzed by unpaired t statistical test. *p ≤ 0.05, **p < 0.01, and ****p < 0.0001.

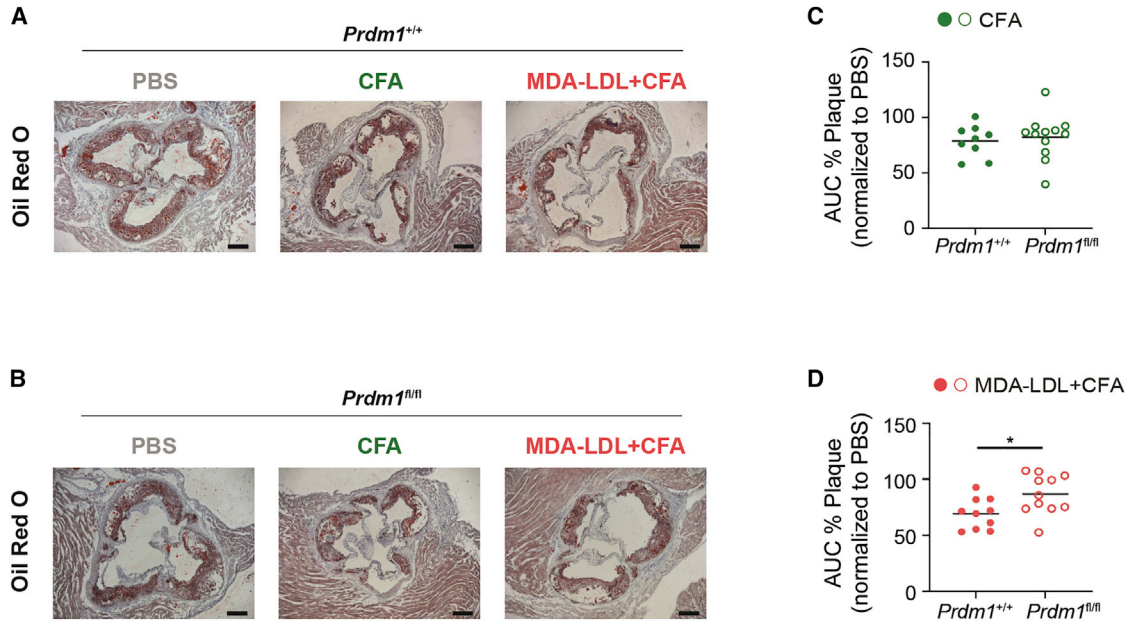

Figure 7. GC-derived PCs and antibodies are required for MDA-LDL immunization-induced athero-protection

(A and B) Representative oil red-O-stained aortic sinus cryosections of (A) *Prdm1*$^{+/+}$ *Aicda*-Cre$^{+/ki}$ *Ldlr*$^{-/-}$ chimeras and (B) *Prdm1*$^{fl/fl}$ *Aicda*-Cre$^{+/ki}$ *Ldlr*$^{-/-}$ chimeras immunized with PBS, CFA, or MDA-LDL + CFA.

(C and D) AUC values of the atherosclerosis quantifications in five serial 80 μm-spaced aortic sinus cryosections from *Prdm1*$^{+/+}$ *Aicda*-Cre$^{+/ki}$ *Ldlr*$^{-/-}$ and *Prdm1*$^{fl/fl}$ *Aicda*-Cre$^{+/ki}$ *Ldlr*$^{-/-}$ chimeras immunized with (C) CFA or (D) MDA-LDL + CFA. Atherosclerosis quantification of CFA- and MDA-LDL + CFA-immunized mice was normalized to the mean AUC value of their respective PBS-injected *Prdm1*$^{+/+}$ *Aicda*-Cre$^{+/ki}$ *Ldlr*$^{-/-}$ and *Prdm1*$^{fl/fl}$ *Aicda*-Cre$^{+/ki}$ *Ldlr*$^{-/-}$ chimeras. All experiments were performed with 8- to 9-week-old male receptors.

Each dot in the graphs represents a biological replicate (individual mouse). Scale bars in images represent 200 μm. Data analyzed by unpaired t statistical test. *$p < 0.05$.

specificities, some of which can have athero-protective properties, while others can aggravate the disease. For instance, anti-ALDH4A1 Abs are athero-protective (Lorenzo et al., 2021), while anti-Hsp60 Abs aggravate atherosclerosis (Foteinos et al., 2005).

In this regard, we have assessed the role of MDA-LDL-specific PCs and/or Abs on atherosclerosis development by MDA-LDL immunization of pro-atherogenic mice under deletion of Blimp1 in GC-derived PCs (*Prdm1*$^{fl/fl}$ *Aicda*-Cre$^{+/ki}$ *Ldlr*$^{-/-}$ chimeras). Depletion of GC-derived PCs dramatically decreased the titers of IgG Abs in MDA-LDL-immunized mice, and MDA-LDL-specific IgG Abs were barely detectable. In contrast, titers of total IgM Abs in MDA-LDL-immunized *Prdm1*$^{fl/fl}$ *Aicda*-Cre$^{+/ki}$ *Ldlr*$^{-/-}$ chimeras remain unchanged compared with PC-proficient mice, and anti-MDA-LDL-specific IgM Abs were only mildly reduced. Therefore, our approach allows a precise study of Ab contribution to MDA-LDL protection because it successfully abolishes the generation of GC-derived, switched Abs while retaining a substantial proportion of IgM Abs, presumably derived from extrafollicular B cell activation. Our results show that MDA-LDL immunization failed to be athero-protective *Prdm1*-deficient chimeras. Thus, our study indicates that MDA-LDL immunization gives rise to athero-protective Abs of GC origin.

Athero-protection by MDA-LDL immunization was first described more than two decades ago (Palinski et al., 1995), opening new therapeutic perspectives based on thorough immunomodulation strategies and most specifically via vaccination strategies using MDA-LDL. However, our limited knowledge on the nature of the immune response to MDA-LDL and its impact on the atherosclerosis process has hindered further progress of this potential therapeutic avenue. Here, we have shown that immunization with MDA-LDL promotes a bona fide GC response and generates MBCs, PCs, and highly mutated anti-MDA-LDL Abs, which are important drivers of MDA-LDL-derived athero-protection. Our data thus indicate that MDA-LDL immunization can warrant a high-affinity, long-lived Ab immune response, possibly comparable to the response elicited by antigens used in vaccination protocols.

Limitations of the study

A limitation of our study is the *Aicda*-Cre$^{+/ki}$ mouse model used to track GC B cells and to deplete Prmd1. As mentioned above, the onset of AID expression shortly precedes the actual entering of the B cell into the follicle, and thus a minor fraction of non-GC B cells could be labeled by our tdTom-based tracing system or be Prdm1 depleted. Nevertheless, this model provides a very good approximation for GC studies because it is very efficient at depleting/labeling GC B cells while having only a minor effect on non-GC cells.

STAR★METHODS

Detailed methods are provided in the online version of this paper and include the following:

- KEY RESOURCES TABLE
- RESOURCE AVAILABILITY

SUPPLEMENTAL INFORMATION

Supplemental information can be found online at https://doi.org/10.1016/j.celrep.2022.111468.

ACKNOWLEDGMENTS

We thank all members of the B Cell Biology Laboratory for useful discussions, A. Rodriguez-Ronchel for the design of the graphical abstract, V.G. de Yébenes for critical reading of the manuscript, and V. Labrador for help with microscopy and image analysis. I.M.-F. and C.L. were fellows of the research training program funded by Ministerio de Economía y Competitividad (SVP-2014-068216 and SVP-2014-068289, respectively), A.d.M.M. is funded by "la Caixa" Foundation HR17–00247, and A.R.R. was supported by Centro Nacional de Investigaciones Cardiovasculares (CNIC). The project leading to these results has received funding from la Caixa Banking Foundation under the project code HR17-00247 and from SAF2016-75511-R and PID2019-106773RB-I00/AEI/10.13039/501100011033 grants to A.R.R. (Plan Estatal de Investigación Científica y Técnica y de Innovación 2013–2016 Programa Estatal de I+D+i Orientada a los Retos de la Sociedad Retos Investigación: Proyectos I + D + i 2016, Ministerio de Economía, Industria y Competitividad) and co-funding by Fondo Europeo de Desarrollo Regional (FEDER). CIBERCV (J.L.M.-V.) and CIBERDEM (J.C.E.-G.) are Instituto de Salud Carlos III projects. The CNIC is supported by the Instituto de Salud Carlos III (ISCIII), the Ministerio de Ciencia e Innovación (MCIN), and the Pro CNIC Foundation and is a Severo Ochoa institute (CEX2020-001041-S grant funded by MCIN/AEI/10.13039/501100011033).

AUTHOR CONTRIBUTIONS

I.M.-F. designed, performed, and analyzed experiments, prepared figures, and wrote the manuscript; A.d.M.M. performed and analyzed experiments and prepared figures; C.L. performed and analyzed experiments; C.E.B. performed and analyzed experiments; P.D. performed and analyzed experiments; L.C.-F. performed experiments; S.M.M. performed experiments; J.C.E.-G. provided reagents; J.L.M.-V. designed experiments; H.W. designed experiments and wrote the manuscript; and A.R.R. conceived the project, designed and analyzed experiments, and wrote the manuscript.

DECLARATION OF INTERESTS

The authors declare no competing interests.

Received: March 31, 2022
Revised: August 13, 2022
Accepted: September 19, 2022
Published: October 11, 2022

REFERENCES

Ait-Oufella, H., Herbin, O., Bouaziz, J.D., Binder, C.J., Uyttenhove, C., Laurans, L., Taleb, S., Van Vré, E., Esposito, B., Vilar, J., et al. (2010). B cell depletion reduces the development of atherosclerosis in mice. J. Exp. Med. *207*, 1579–1587. https://doi.org/10.1084/jem.20100155.

Ait-Oufella, H., Salomon, B.L., Potteaux, S., Robertson, A.K.L., Gourdy, P., Zoll, J., Merval, R., Esposito, B., Cohen, J.L., Fisson, S., et al. (2006). Natural regulatory T cells control the development of atherosclerosis in mice. Nat. Med. *12*, 178–180. https://doi.org/10.1038/nm1343.

Albright, A.R., Kabat, J., Li, M., Raso, F., Reboldi, A., and Muppidi, J.R. (2019). TGFbeta signaling in germinal center B cells promotes the transition from light zone to dark zone. J. Exp. Med. *216*, 2531–2545. https://doi.org/10.1084/jem.20181868.

Almanzar, G., Öllinger, R., Leuenberger, J., Onestingel, E., Rantner, B., Zehm, S., Cardini, B., van der Zee, R., Grundtman, C., and Wick, G. (2012). Autoreactive HSP60 epitope-specific T-cells in early human atherosclerotic lesions. J. Autoimmun. *39*, 441–450. https://doi.org/10.1016/j.jaut.2012.07.006.

Binder, C.J., Hartvigsen, K., Chang, M.K., Miller, M., Broide, D., Palinski, W., Curtiss, L.K., Corr, M., and Witztum, J.L. (2004). IL-5 links adaptive and natural immunity specific for epitopes of oxidized LDL and protects from atherosclerosis. J. Clin. Invest. *114*, 427–437. https://doi.org/10.1172/JCI20479.

Bobryshev, Y.V., Ivanova, E.A., Chistiakov, D.A., Nikiforov, N.G., and Orekhov, A.N. (2016). Macrophages and their role in atherosclerosis: pathophysiology and transcriptome analysis. BioMed Res. Int. *2016*, 9582430. https://doi.org/10.1155/2016/9582430.

Brophy, M.L., Dong, Y., Wu, H., Rahman, H.N.A., Song, K., and Chen, H. (2017). Eating the Dead to keep atherosclerosis at bay. Front. Cardiovasc. Med. *4*, 2. https://doi.org/10.3389/fcvm.2017.00002.

Busse, C.E., Czogiel, I., Braun, P., Arndt, P.F., and Wardemann, H. (2014). Single-cell based high-throughput sequencing of full-length immunoglobulin heavy and light chain genes. Eur. J. Immunol. *44*, 597–603. https://doi.org/10.1002/eji.201343917.

Caligiuri, G., Nicoletti, A., Poirier, B., and Hansson, G.K. (2002). Protective immunity against atherosclerosis carried by B cells of hypercholesterolemic mice. J. Clin. Invest. *109*, 745–753. https://doi.org/10.1172/JCI7272.

Cedó, L., Metso, J., Santos, D., García-León, A., Plana, N., Sabate-Soler, S., Rotllan, N., Rivas-Urbina, A., Méndez-Lara, K.A., Tondo, M., et al. (2020). LDL receptor regulates the reverse transport of macrophage-derived unesterified cholesterol via concerted action of the HDL-LDL Axis: insight from mouse models. Circ. Res. *127*, 778–792. https://doi.org/10.1161/CIRCRESAHA.119.316424.

Centa, M., Jin, H., Hofste, L., Hellberg, S., Busch, A., Baumgartner, R., Verzaal, N.J., Lind Enoksson, S., Perisic Matic, L., Boddul, S.V., et al. (2019). Germinal center-derived antibodies promote atherosclerosis plaque size and stability. Circulation *139*, 2466–2482. https://doi.org/10.1161/CIRCULATIONAHA.118.038534.

Clement, M., Guedj, K., Andreata, F., Morvan, M., Bey, L., Khallou-Laschet, J., Gaston, A.T., Delbosc, S., Alsac, J.M., Bruneval, P., et al. (2015). Control of the T follicular helper-germinal center B-cell axis by CD8(+) regulatory T cells limits atherosclerosis and tertiary lymphoid organ development. Circulation *131*, 560–570. https://doi.org/10.1161/CIRCULATIONAHA.114.010988.

Foteinos, G., Afzal, A.R., Mandal, K., Jahangiri, M., and Xu, Q. (2005). Anti-heat shock protein 60 autoantibodies induce atherosclerosis in apolipoprotein E-deficient mice via endothelial damage. Circulation *112*, 1206–1213. https://doi.org/10.1161/CIRCULATIONAHA.105.547414.

Fredrikson, G.N., Soderberg, I., Lindholm, M., Dimayuga, P., Chyu, K.Y., Shah, P.K., and Nilsson, J. (2003). Inhibition of atherosclerosis in apoE-null mice by immunization with apoB-100 peptide sequences. Arterioscler. Thromb. Vasc. Biol. *23*, 879–884. https://doi.org/10.1161/01.ATV.0000067937.93716.

Freigang, S., Hörkkö, S., Miller, E., Witztum, J.L., and Palinski, W. (1998). Immunization of LDL receptor-deficient mice with homologous malondialdehyde-modified and native LDL reduces progression of atherosclerosis by mechanisms other than induction of high titers of antibodies to oxidative

neoepitopes. Arterioscler. Thromb. Vasc. Biol. *18*, 1972–1982. https://doi.org/10.1161/01.atv.18.12.1972.

George, J., Afek, A., Gilburd, B., Levkovitz, H., Shaish, A., Goldberg, I., Kopolovic, Y., Wick, G., Shoenfeld, Y., and Harats, D. (1998). Hyperimmunization of apo-E-deficient mice with homologous malondialdehyde low-density lipoprotein suppresses early atherogenesis. Atherosclerosis *138*, 147–152. https://doi.org/10.1016/s0021-9150(98)00015-x.

George, J., Shoenfeld, Y., Afek, A., Gilburd, B., Keren, P., Shaish, A., Kopolovic, J., Wick, G., and Harats, D. (1999). Enhanced fatty streak formation in C57BL/6J mice by immunization with heat shock protein-65. Arterioscler. Thromb. Vasc. Biol. *19*, 505–510. https://doi.org/10.1161/01.atv.19.3.505.

Gisterå, A., Klement, M.L., Polyzos, K.A., Mailer, R.K.W., Duhlin, A., Karlsson, M.C.I., Ketelhuth, D.F.J., and Hansson, G.K. (2018). Low-density lipoprotein-reactive T cells regulate plasma cholesterol levels and development of atherosclerosis in humanized hypercholesterolemic mice. Circulation *138*, 2513–2526. https://doi.org/10.1161/CIRCULATIONAHA.118.034076.

Gitlin, A.D., von Boehmer, L., Gazumyan, A., Shulman, Z., Oliveira, T.Y., and Nussenzweig, M.C. (2016). Independent roles of switching and hypermutation in the development and persistence of B lymphocyte memory. Immunity *44*, 769–781. https://doi.org/10.1016/j.immuni.2016.01.011.

Gómez-Escolar, C., Serrano-Navarro, A., Benguria, A., Dopazo, A., Sánchez-Cabo, F., and Ramiro, A.R. (2021). Single cell clonal analysis identifies an AID-dependent pathway of plasma cell differentiation. Preprint at bioRxiv. https://doi.org/10.1101/2021.06.03.446763.

Grasset, E.K., Duhlin, A., Agardh, H.E., Ovchinnikova, O., Hägglöf, T., Forsell, M.N., Paulsson-Berne, G., Hansson, G.K., Ketelhuth, D.F.J., and Karlsson, M.C.I. (2015). Sterile inflammation in the spleen during atherosclerosis provides oxidation-specific epitopes that induce a protective B-cell response. Proc. Natl. Acad. Sci. USA *112*, E2030–E2038. https://doi.org/10.1073/pnas.1421227112.

Gupta, S., Pablo, A.M., Jiang, X.c., Wang, N., Tall, A.R., and Schindler, C. (1997). IFN-gamma potentiates atherosclerosis in ApoE knock-out mice. J. Clin. Invest. *99*, 2752–2761. https://doi.org/10.1172/JCI119465.

Hansen, P.R., Chew, M., Zhou, J., Daugherty, A., Heegaard, N., Jensen, P., Mouritsen, S., and Falk, E. (2001). Freunds adjuvant alone is antiatherogenic in apoE-deficient mice and specific immunization against TNFalpha confers no additional benefit. Atherosclerosis *158*, 87–94. https://doi.org/10.1016/s0021-9150(01)00418-x.

Hansson, G.K., and Hermansson, A. (2011). The immune system in atherosclerosis. Nat. Immunol. *12*, 204–212. https://doi.org/10.1038/ni.2001.

Hansson, G.K., Holm, J., and Jonasson, L. (1989). Detection of activated T lymphocytes in the human atherosclerotic plaque. Am. J. Pathol. *135*, 169–175.

Hansson, G.K., Robertson, A.K.L., and Söderberg-Nauclér, C. (2006). Inflammation and atherosclerosis. Annu. Rev. Pathol. *1*, 297–329. https://doi.org/10.1146/annurev.pathol.1.110304.100100.

Hartley, A., Haskard, D., and Khamis, R. (2019). Oxidized LDL and anti-oxidized LDL antibodies in atherosclerosis - novel insights and future directions in diagnosis and therapy<sup/&gt. Trends Cardiovasc. Med. *29*, 22–26. https://doi.org/10.1016/j.tcm.2018.05.010.

Hjerpe, C., Johansson, D., Hermansson, A., Hansson, G.K., and Zhou, X. (2010). Dendritic cells pulsed with malondialdehyde modified low density lipoprotein aggravate atherosclerosis in Apoe(-/-) mice. Atherosclerosis *209*, 436–441. https://doi.org/10.1016/j.atherosclerosis.2009.10.003.

Hollander, W., Colombo, M.A., Kirkpatrick, B., and Paddock, J. (1979). Soluble proteins in the human atherosclerotic plaque. With spectral reference to immunoglobulins, C3-complement component, alpha 1-antitrypsin and alpha 2-macroglobulin. Atherosclerosis *34*, 391–405. https://doi.org/10.1016/0021-9150(79)90064-9.

Imkeller, K., Arndt, P.F., Wardemann, H., and Busse, C.E. (2016). sciReptor: analysis of single-cell level immunoglobulin repertoires. BMC Bioinf. *17*, 67. https://doi.org/10.1186/s12859-016-0920-1.

Ishibashi, S., Brown, M.S., Goldstein, J.L., Gerard, R.D., Hammer, R.E., and Herz, J. (1993). Hypercholesterolemia in low density lipoprotein receptor knockout mice and its reversal by adenovirus-mediated gene delivery. J Clin Invest *92*, 883–893. https://doi.org/10.1172/JCI116663.

Jonasson, L., Holm, J., Skalli, O., Bondjers, G., and Hansson, G.K. (1986). Regional accumulations of T cells, macrophages, and smooth muscle cells in the human atherosclerotic plaque. Arteriosclerosis *6*, 131–138. https://doi.org/10.1161/01.atv.6.2.131.

Karvonen, J., Päivänsalo, M., Kesäniemi, Y.A., and Hörkkö, S. (2003). Immunoglobulin M type of autoantibodies to oxidized low-density lipoprotein has an inverse relation to carotid artery atherosclerosis. Circulation *108*, 2107–2112. https://doi.org/10.1161/01.CIR.0000092891.55157.A7.

Kyaw, T., Cui, P., Tay, C., Kanellakis, P., Hosseini, H., Liu, E., Rolink, A.G., Tipping, P., Bobik, A., and Toh, B.H. (2013). BAFF receptor mAb treatment ameliorates development and progression of atherosclerosis in hyperlipidemic ApoE(-/-) mice. PLoS One *8*, e60430. https://doi.org/10.1371/journal.pone.0060430.

Kyaw, T., Tay, C., Khan, A., Dumouchel, V., Cao, A., To, K., Kehry, M., Dunn, R., Agrotis, A., Tipping, P., et al. (2010). Conventional B2 B cell depletion ameliorates whereas its adoptive transfer aggravates atherosclerosis. J. Immunol. *185*, 4410–4419. https://doi.org/10.4049/jimmunol.1000033.

Kyaw, T., Tay, C., Krishnamurthi, S., Kanellakis, P., Agrotis, A., Tipping, P., Bobik, A., and Toh, B.H. (2011). B1a B lymphocytes are atheroprotective by secreting natural IgM that increases IgM deposits and reduces necrotic cores in atherosclerotic lesions. Circ. Res. *109*, 830–840. https://doi.org/10.1161/CIRCRESAHA.111.248542.

Lahoute, C., Herbin, O., Mallat, Z., and Tedgui, A. (2011). Adaptive immunity in atherosclerosis: mechanisms and future therapeutic targets. Nat. Rev. Cardiol. *8*, 348–358. https://doi.org/10.1038/nrcardio.2011.62.

Lehrer-Graiwer, J., Singh, P., Abdelbaky, A., Vucic, E., Korsgren, M., Baruch, A., Fredrickson, J., van Bruggen, N., Tang, M.T., Frendeus, B., et al. (2015). FDG-PET imaging for oxidized LDL in stable atherosclerotic disease: a phase II study of safety, tolerability, and anti-inflammatory activity. JACC. Cardiovasc. Imaging *8*, 493–494. https://doi.org/10.1016/j.jcmg.2014.06.021.

Libby, P. (2021). The changing landscape of atherosclerosis. Nature *592*, 524–533. https://doi.org/10.1038/s41586-021-03392-8.

Lorenzo, C., Delgado, P., Busse, C.E., Sanz-Bravo, A., Martos-Folgado, I., Bonzon-Kulichenko, E., Ferrarini, A., Gonzalez-Valdes, I.B., Mur, S.M., Roldán-Montero, R., et al. (2021). ALDH4A1 is an atherosclerosis auto-antigen targeted by protective antibodies. Nature *589*, 287–292. https://doi.org/10.1038/s41586-020-2993-2.

Lusis, A.J. (2000). Nature *407*, 233–241. https://doi.org/10.1038/35025203.

Madisen, L., Zwingman, T.A., Sunkin, S.M., Oh, S.W., Zariwala, H.A., Gu, H., Ng, L.L., Palmiter, R.D., Hawrylycz, M.J., Jones, A.R., et al. (2010). A robust and high-throughput Cre reporting and characterization system for the whole mouse brain. Nat. Neurosci. *13*, 133–140. https://doi.org/10.1038/nn.2467.

Major, A.S., Fazio, S., and Linton, M.F. (2002). B-lymphocyte deficiency increases atherosclerosis in LDL receptor-null mice. Arterioscler. Thromb. Vasc. Biol. *22*, 1892–1898. https://doi.org/10.1161/01.atv.0000039169.47943.ee.

Mayer, C.T., Nieke, J.P., Gazumyan, A., Cipolla, M., Wang, Q., Oliveira, T.Y., Ramos, V., Monette, S., Li, Q.Z., Gershwin, M.E., et al. (2020). An apoptosis-dependent checkpoint for autoimmunity in memory B and plasma cells. Proc. Natl. Acad. Sci. USA *117*, 24957–24963. https://doi.org/10.1073/pnas.2015372117.

Murugan, R., Imkeller, K., Busse, C.E., and Wardemann, H. (2015). Direct high-throughput amplification and sequencing of immunoglobulin genes from single human B cells. Eur. J. Immunol. *45*, 2698–2700. https://doi.org/10.1002/eji.201545526.

Nilsson, J., and Hansson, G.K. (2020). Vaccination strategies and immune modulation of atherosclerosis. Circ. Res. *126*, 1281–1296. https://doi.org/10.1161/CIRCRESAHA.120.315942.

Nus, M., Sage, A.P., Lu, Y., Masters, L., Lam, B.Y.H., Newland, S., Weller, S., Tsiantoulas, D., Raffort, J., Marcus, D., et al. (2017). Marginal zone B cells control the response of follicular helper T cells to a high-cholesterol diet. Nat. Med. *23*, 601–610. https://doi.org/10.1038/nm.4315.

Palinski, W., Miller, E., and Witztum, J.L. (1995). Immunization of low density lipoprotein (LDL) receptor-deficient rabbits with homologous malondialdehyde-modified LDL reduces atherogenesis. Proc. Natl. Acad. Sci. USA *92*, 821–825. https://doi.org/10.1073/pnas.92.3.821.

Palinski, W., Ord, V.A., Plump, A.S., Breslow, J.L., Steinberg, D., and Witztum, J.L. (1994). ApoE-deficient mice are a model of lipoprotein oxidation in atherogenesis. Demonstration of oxidation-specific epitopes in lesions and high titers of autoantibodies to malondialdehyde-lysine in serum. Arterioscler. Thromb. *14*, 605–616. https://doi.org/10.1161/01.atv.14.4.605.

Palinski, W., Rosenfeld, M.E., Ylä-Herttuala, S., Gurtner, G.C., Socher, S.S., Butler, S.W., Parthasarathy, S., Carew, T.E., Steinberg, D., and Witztum, J.L. (1989). Low density lipoprotein undergoes oxidative modification in vivo. Proc. Natl. Acad. Sci. USA *86*, 1372–1376. https://doi.org/10.1073/pnas.86.4.1372.

Palinski, W., Ylä-Herttuala, S., Rosenfeld, M.E., Butler, S.W., Socher, S.A., Parthasarathy, S., Curtiss, L.K., and Witztum, J.L. (1990). Antisera and monoclonal antibodies specific for epitopes generated during oxidative modification of low density lipoprotein. Arteriosclerosis *10*, 325–335. https://doi.org/10.1161/01.atv.10.3.325.

Robbiani, D.F., Bothmer, A., Callen, E., Reina-San-Martin, B., Dorsett, Y., Difilippantonio, S., Bolland, D.J., Chen, H.T., Corcoran, A.E., Nussenzweig, A., and Nussenzweig, M.C. (2008). AID is required for the chromosomal breaks in c-myc that lead to c-myc/IgH translocations. Cell *135*, 1028–1038. https://doi.org/10.1016/j.cell.2008.09.062.

Rommel, P.C., Bosque, D., Gitlin, A.D., Croft, G.F., Heintz, N., Casellas, R., Nussenzweig, M.C., Kriaucionis, S., and Robbiani, D.F. (2013). Fate mapping for activation-induced cytidine deaminase (AID) marks non-lymphoid cells during mouse development. PLoS One *8*, e69208. https://doi.org/10.1371/journal.pone.0069208.

Rosenfeld, S.M., Perry, H.M., Gonen, A., Prohaska, T.A., Srikakulapu, P., Grewal, S., Das, D., McSkimming, C., Taylor, A.M., Tsimikas, S., et al. (2015). B-1b cells secrete atheroprotective IgM and attenuate atherosclerosis. Circ. Res. *117*, e28–e39. https://doi.org/10.1161/CIRCRESAHA.117.306044.

Sage, A.P., Nus, M., Bagchi Chakraborty, J., Tsiantoulas, D., Newland, S.A., Finigan, A.J., Masters, L., Binder, C.J., and Mallat, Z. (2017). X-box binding protein-1 dependent plasma cell responses limit the development of atherosclerosis. Circ. Res. *121*, 270–281. https://doi.org/10.1161/CIRCRESAHA.117.310884.

Sage, A.P., Tsiantoulas, D., Baker, L., Harrison, J., Masters, L., Murphy, D., Loinard, C., Binder, C.J., and Mallat, Z. (2012). BAFF receptor deficiency reduces the development of atherosclerosis in mice–brief report. Arterioscler. Thromb. Vasc. Biol. *32*, 1573–1576. https://doi.org/10.1161/ATVBAHA.111.244731.

Saigusa, R., Winkels, H., and Ley, K. (2020). T cell subsets and functions in atherosclerosis. Nat. Rev. Cardiol. *17*, 387–401. https://doi.org/10.1038/s41569-020-0352-5.

Shaffer, A.L., Lin, K.I., Kuo, T.C., Yu, X., Hurt, E.M., Rosenwald, A., Giltnane, J.M., Yang, L., Zhao, H., Calame, K., and Staudt, L.M. (2002). Blimp-1 orchestrates plasma cell differentiation by extinguishing the mature B cell gene expression program. Immunity *17*, 51–62. https://doi.org/10.1016/s1074-7613(02)00335-7.

Shapiro-Shelef, M., Lin, K.I., McHeyzer-Williams, L.J., Liao, J., McHeyzer-Williams, M.G., and Calame, K. (2003). Blimp-1 is required for the formation of immunoglobulin secreting plasma cells and pre-plasma memory B cells. Immunity *19*, 607–620. https://doi.org/10.1016/s1074-7613(03)00267-x.

Shaw, P.X., Hörkkö, S., Chang, M.K., Curtiss, L.K., Palinski, W., Silverman, G.J., and Witztum, J.L. (2000). Natural antibodies with the T15 idiotype may act in atherosclerosis, apoptotic clearance, and protective immunity. J. Clin. Invest. *105*, 1731–1740. https://doi.org/10.1172/JCI8472.

Skålén, K., Gustafsson, M., Rydberg, E.K., Hultén, L.M., Wiklund, O., Innerarity, T.L., and Borén, J. (2002). Subendothelial retention of atherogenic lipoproteins in early atherosclerosis. Nature *417*, 750–754. https://doi.org/10.1038/nature00804.

Tabas, I., Williams, K.J., and Borén, J. (2007). Subendothelial lipoprotein retention as the initiating process in atherosclerosis: update and therapeutic implications. Circulation *116*, 1832–1844. https://doi.org/10.1161/CIRCULATIONAHA.106.676890.

Talayero, B.G., and Sacks, F.M. (2011). The role of triglycerides in atherosclerosis. Curr. Cardiol. Rep. *13*, 544–552. https://doi.org/10.1007/s11886-011-0220-3.

Tay, C., Liu, Y.H., Kanellakis, P., Kallies, A., Li, Y., Cao, A., Hosseini, H., Tipping, P., Toh, B.H., Bobik, A., and Kyaw, T. (2018). Follicular B cells promote atherosclerosis via T cell-mediated differentiation into plasma cells and secreting pathogenic immunoglobulin G. Arterioscler. Thromb. Vasc. Biol. *38*, e71–e84. https://doi.org/10.1161/ATVBAHA.117.310678.

Tsimikas, S., Brilakis, E.S., Lennon, R.J., Miller, E.R., Witztum, J.L., McConnell, J.P., Kornman, K.S., and Berger, P.B. (2007). Relationship of IgG and IgM autoantibodies to oxidized low density lipoprotein with coronary artery disease and cardiovascular events. J. Lipid Res. *48*, 425–433. https://doi.org/10.1194/jlr.M600361-JLR200.

Turunen, S.P., Kummu, O., Wang, C., Harila, K., Mattila, R., Sahlman, M., Pussinen, P.J., and Hörkkö, S. (2015). Immunization with malondialdehyde-modified low-density lipoprotein (LDL) reduces atherosclerosis in LDL receptor-deficient mice challenged with Porphyromonas gingivalis. Innate Immun. *21*, 370–385. https://doi.org/10.1177/1753425914542444.

Venegas-Pino, D.E., Banko, N., Khan, M.I., Shi, Y., and Werstuck, G.H. (2013). Quantitative analysis and characterization of atherosclerotic lesions in the murine aortic sinus. J. Vis. Exp., 50933. https://doi.org/10.3791/50933.

Weisel, F.J., Zuccarino-Catania, G.V., Chikina, M., and Shlomchik, M.J. (2016). A temporal Switch in the germinal center determines differential output of memory B and plasma cells. Immunity *44*, 116–130. https://doi.org/10.1016/j.immuni.2015.12.004.

Xu, Q., Dietrich, H., Steiner, H.J., Gown, A.M., Schoel, B., Mikuz, G., Kaufmann, S.H., and Wick, G. (1992). Induction of arteriosclerosis in normocholesterolemic rabbits by immunization with heat shock protein 65. Arterioscler. Thromb. *12*, 789–799. https://doi.org/10.1161/01.atv.12.7.789.

Xu, Q., Willeit, J., Marosi, M., Kleindienst, R., Oberhollenzer, F., Kiechl, S., Stulnig, T., Luef, G., and Wick, G. (1993). Association of serum antibodies to heat-shock protein 65 with carotid atherosclerosis. Lancet *341*, 255–259. https://doi.org/10.1016/0140-6736(93)92613-x.

Ylä-Herttuala, S., Palinski, W., Rosenfeld, M.E., Parthasarathy, S., Carew, T.E., Butler, S., Witztum, J.L., and Steinberg, D. (1989). Evidence for the presence of oxidatively modified low density lipoprotein in atherosclerotic lesions of rabbit and man. J. Clin. Invest. *84*, 1086–1095. https://doi.org/10.1172/JCI114271.

Zeng, Z., Cao, B., Guo, X., Li, W., Li, S., Chen, J., Zhou, W., Zheng, C., and Wei, Y. (2018). Apolipoprotein B-100 peptide 210 antibody inhibits atherosclerosis by regulation of macrophages that phagocytize oxidized lipid. Am. J. Transl. Res. *10*, 1817–1828.

Zhou, X., Caligiuri, G., Hamsten, A., Lefvert, A.K., and Hansson, G.K. (2001). LDL immunization induces T-cell-dependent antibody formation and protection against atherosclerosis. Arterioscler. Thromb. Vasc. Biol. *21*, 108–114. https://doi.org/10.1161/01.atv.21.1.108.

Zhou, X., Robertson, A.K.L., Rudling, M., Parini, P., and Hansson, G.K. (2005). Lesion development and response to immunization reveal a complex role for CD4 in atherosclerosis. Circ. Res. *96*, 427–434. https://doi.org/10.1161/01.RES.0000156889.22364.f1.

Zhu, J., Quyyumi, A.A., Rott, D., Csako, G., Wu, H., Halcox, J., and Epstein, S.E. (2001). Antibodies to human heat-shock protein 60 are associated with the presence and severity of coronary artery disease: evidence for an autoimmune component of atherogenesis. Circulation *103*, 1071–1075. https://doi.org/10.1161/01.cir.103.8.1071.

STAR★METHODS

KEY RESOURCES TABLE

REAGENT or RESOURCE	SOURCE	IDENTIFIER
Antibodies		
anti-mouse CD16/CD32 (clone 2.4G2)	BD Pharmingen	Cat#553142; RRID: AB_394657
anti-mouse B220 (clone RA3-6B2)	BD Horizon	Cat#562922; RRID: AB_2737894
anti-mouse GL7 (clone GL7)	Biolegend	Cat#144610; RRID: AB_2562979
anti-mouse PD-L2 (clone TY25)	BD Biosciences	Cat#560086; RRID: AB_1645223
anti-mouse CD138 (clone 281-2)	BD Biosciences	Cat#563193; RRID: AB_2738060
anti-mouse IgD (clone 11–26)	SouthernBiotech	Cat#553439; RRID: AB_394859
anti-mouse IgG1 (clone A85-1)	BD Pharmingen	Cat#553441; RRID: AB_394861
anti-mouse IgG2B (clone RMG2b-1)	BioLegend	Cat#406706; RRID: AB_493297
anti-mouse IgM (clone IL/41)	BD Pharmingen	Cat#553437; RRID: AB_394857
anti-mouse CD45.1 (clone A20)	Tonbo	Cat#65043U100
anti-mouse CD45.2 (clone 104)	BD Pharmingen	Cat#563686
anti-mouse CD3 (clone 145-2C11)	BD Biosciences	Cat#553062; RRID: AB_394595
anti-mouse CD19 (clone 145-2C11)	BD Pharmingen	Cat#557399; RRID: AB_396682
Goat anti-Mouse IgG1 Antibody HRP Conjugated	Bethyl	Cat#A90-105P; RRID: AB_67150
Goat anti-Mouse IgG2b Antibody HRP Conjugated	Bethyl	Cat#A90-109P; RRID: AB_67160
Goat anti-Mouse IgG2c Antibody HRP Conjugated	Bethyl	Cat#A90-136P; RRID: AB_67165
anti-mouse B220 (clone RA3-6B2)	BD Biosciences	Cat#553088; RRID: AB_394618
anti-mouse SMA-1 (clone 1A4)	Thermo Fisher Scientific	Cat#MA511547; RRID: AB_10979529
anti-mouse MAC-2 (clone M3/38)	Cedarlane	Cat#CL8942AP; RRID: AB_10060357
Goat anti-Rat IgG, Alexa Fluor™ 568	Thermo Fisher Scientific	Cat#A-11077; RRID: AB_10060357
Biological samples		
Human LDL	Joan Carles Escolà-Gil	N/A
Chemicals, peptides, and recombinant proteins		
Malondialdehyde bis (dimethyl acetal)	Sigma-Aldrich	Cat#8207560005
Adjuvant Complete Freunds (CFA)	BD Biosciences	Cat#210485
Adjuvant Incomplete Freunds (IFA)	BD Biosciences	Cat#210486
Bovine Serum Albumin (BSA)	Sigma-Aldrich	Cat#A9418
7AAD	BD Pharmingen	Cat# 559925
LIVE/DEAD® Fixable Yellow Dead Cell Stain Kit	Thermo Fisher Scientific	Cat#L34967
TMB substrate	Bethyl	Cat#E102
OCT Compound	Sakura	Cat#4583
Mayer's hematoxylin	Bio-Optica	Cat#05–06002/L
Oil Red-O	MERCK	Cat#S0389
Picrosirius	Riedel-de haë	Cat#4248
Amonium chloride	Sigma-Aldrich	Cat#A9434
Triton X-100	Sigma-Aldrich	Cat#T9284
Lectin PNA, Alexa Fluor™ 647 Conjugate	Thermo Fisher Scientific	Cat# L32460
DAPI	Sigma-Aldrich	Cat#D9542
Prolong Gold	Life Technologies	Cat#P36930
Critical commercial assays		
PD10 desalting columns	Sigma-Aldrich	Cat#GE17-0851-01
Mouse IgM ELISA Quantitation Set	Bethyl	Cat#E90-101
Mouse IgG ELISA Quantitation Set	Bethyl	Cat#E90-131

(*Continued on next page*)

Continued		
REAGENT or RESOURCE	SOURCE	IDENTIFIER
Avidin/Biotin blocking kit	Vector Labs	Cat#SP-2001
Experimental models: Organisms/strains		
Mouse: *Ldlr*$^{-/-}$, 8–28 weeks old 8 (see figure legends for details on specific experiments)	Jackson laboratories	Cat#002207
Mouse: *Aicda*$^{Cre/+}$, 6–8 weeks old	Jackson laboratories	Cat#007770
Mouse: *Rosa26tdTomato*$^{+/ki}$, 6–8 weeks old	Jackson laboratories	Cat#007909
Mouse: *Prdm1*$^{+/fl}$, 8–13 weeks old	Jackson laboratories	Cat#008100
Oligonucleotides		
Igh 1° PCR: mIghd-114-rv, 5′-CAGAGGGGA AGACATGTTCAACTAT-3′	This paper	N/A
Igh 2° PCR: mIghd-079-rv, 5′-CAGTGGCTG ACTTCCAATTACTAAAC-3′	This paper	N/A
Software and algorithms		
FlowJo – version 10	FlowJo, LLC	https://www.flowjo.com/solutions/flowjo/
sciReptor version v1.1-2-gf4cf8e2	Imkeller et al., 2016	N/A
Prism – version 8	GraphPad	https://www.graphpad.com/scientificsoftware/prism
Image J	https://doi.org/10.1038/nmeth.2089	https://imagej.nih.gov/ij/

RESOURCE AVAILABILITY

Lead contact

Further information and requests for resources and reagents should be directed to and will be fulfilled by the lead contact, Almudena R. Ramiro (aramiro@cnic.es).

Materials availability

Materials generated in this study will be made available upon request after signing a materials transfer agreement with CNIC.

Data and code availability

- Data generated in the study are included in the manuscript.
- Any additional information will be shared upon request to the lead contact.
- The study does not report original code.

EXPERIMENTAL MODELS AND SUBJECT DETAILS

Mice

Mice aged 6–28 weeks old were used in the experiments. *Ldlr*$^{-/-}$ mice were originally obtained from Jackson Laboratories (002207) (Ishibashi et al., 1993). *Aicda*-Cre$^{+/ki}$ *R26tdTom*$^{+/ki}$ mice were generated by crossing *Aicda*-Cre$^{+/ki}$ mice obtained from Jackson Laboratories (007770) (Robbiani et al., 2008) with *R26tdTomato*$^{+/ki}$ mice acquired from Jackson Laboratories (007914) (Madisen et al., 2010). *Prdm1*$^{+/fl}$ mice were acquired from Jackson Laboratories (008100) (Shapiro-Shelef et al., 2003) and crossed with *Aicda*-Cre$^{+/ki}$ mice to generate *Prdm1*$^{fl/fl}$ *Aicda*-Cre$^{+/ki}$ and control *Prdm1*$^{+/+}$ *Aicda*-Cre$^{+/ki}$ mice. *Ldlr*$^{-/-}$ males were used for atherosclerosis experiments (Figure 1, and host *Ldlr*$^{-/-}$ for BMT experiments in Figures 6 and 7) in order to reduce the variability of atherosclerosis progression between males and females. Both males and females were used in the rest of the experiments. For MDA-LDL athero-protection experiments, mice were fed with HFD containing 21% of crude fat and 1% cholesterol and/or with HFD containing 21% of crude fat and 1.25% cholesterol (EF D12079 mod. 1% chol and EF D12079 mod. 1.25% chol, Ssniff Spezialdiäten, respectively). In the rest of atherosclerosis experiments, mice were fed with a HFD containing 21% of crude fat and 0.2% cholesterol (EF D12079, Ssniff Spezialdiäten). All animals were housed at the CNIC animal facility under a 12 h dark/light cycle with food and water ad libitum. All animal procedures were approved by the CNIC Ethics Committee and the Madrid regional authorities (PROEX 377/15) and conformed to EU Directive 2010/63/EU and Recommendation 2007/526/EC regarding the protection of animals used for experimental and other scientific purposes, enforced in Spanish law under Real Decreto 1201/2005.

METHOD DETAILS

Antigen preparation and immunization protocols

LDL was isolated as previously described (Cedo et al., 2020). In brief, pooled plasma from healthy donors was mixed with different densities potassium bromide solutions and sequentially ultracentrifugated. The LDL fraction was then isolated at a density of 1.019–1.063 g/mL and dialyzed in PBS. MDA-LDL and MDA-BSA were prepared as described (Palinski et al., 1990). Briefly, LDL or BSA (Sigma-Aldrich) were incubated with 0.5M MDA in a ratio of 100 μL MDA/mg LDL during 3 h at 37°C. 0.5 M MDA was freshly prepared by acid hydrolysis of malonaldehyde bis dimethylacetal (Sigma-Aldrich). After incubation, MDA-LDL and MDA-BSA were purified using PD10 desalting columns following the manufacturer's protocol (Sigma-Aldrich, GE17-0851-01). In athero-protection experiments, 21–28-week-old LDLR$^{-/-}$ mice and 14-18-week-old *Prdm1*$^{+/+}$ *Aicda*-Cre$^{+/ki}$ *Ldlr*$^{-/-}$ and *Prdm1*$^{fl/fl}$ *Aicda*-Cre$^{+/ki}$ *Ldlr*$^{-/-}$ chimeras were immunized subcutaneously (footpads) with 50 μg of MDA-LDL (25 μg/footpad) emulsified in complete Freund's Adjuvant (CFA) in a 1:1 ratio. Booster immunizations were performed 4 times every 2 weeks and 3 times more monthly, injecting 25 μg of MDA-LDL emulsified in incomplete Freund's Adjuvant (IFA) intraperitoneally. In MDA-LDL immunization kinetics analysis, 7-10-week-old *Aicda*-Cre$^{+/ki}$ *R26tdTom*$^{+/ki}$ mice, were immunized as described above. Control mice were injected with PBS emulsified in CFA or IFA (1:1).

Flow cytometry

Single-cell suspensions were obtained from lymph nodes, spleen and bone marrow. After erythrocyte lysis, Fc receptors were blocked with anti-mouse CD16/CD32 antibodies and stained with fluorophore or biotin-conjugated anti-mouse antibodies (BD Pharmingen, Biolegend, Tonbo or eBioscience) to detect B220 (RA3-6B2), GL7 (GL-7), PD-L2 (TY25), CD138 (281-2), IgD (11–26), IgG1 (A85-1), IgG2b (RMG2b-1), IgM (IL/41), CD45.1 (A20), CD45.2 (104), CD3 (145-2C11), CD19 (1D3). Fluorophore-conjugated streptavidin (BD) was used to detect biotin-conjugated antibodies. For live cells detection, staining with 7AAD (BD Pharmingen) or LIVE/DEAD Fixable Yellow Dead Cell Stain (Thermo Fisher) was performed. Samples were acquired on LSRFortessa or FACSCanto instruments (BD Biosciences) and analyzed with FlowJo V10.4.2 software.

Bone marrow transfer

CD45.1 *Ldlr*$^{-/-}$ mice were lethally irradiated with two doses of 5.5 Gy. The following day, femurs and tibias from CD45.2 *Prdm1*$^{+/+}$ *Aicda*-Cre$^{+/ki}$ and CD45.2 *Prdm1*$^{fl/fl}$ *Aicda*-Cre$^{+/ki}$ mice were harvested and processed to obtain bone marrow cell suspension. 8 to 10 × 10^6 bone marrow pooled cells from each genotype donors were transferred intravenously into lethally irradiated *Ldlr*$^{-/-}$ recipient mice. Four weeks after transplantation, bone marrow reconstitution was checked in blood using the CD45.1 and CD45.2 haplotypes as markers to detect donor and recipient cells.

Single-cell sorting and sequencing of immunoglobulin transcripts

Single cell sorting, and primer matrix-based Ig gene single cell PCR and sequencing were performed as previously described (Busse et al., 2014; Murugan et al., 2015). Briefly, GC B cells (B220$^+$ GL7$^+$ tdTom$^+$) and MBCs (B220$^+$ GL7$^-$ tdTom$^+$) from lymph nodes and plasma cells PCs (CD138$^+$tdTom$^+$) from bone marrow were isolated from CFA and MDA-LDL + CFA immunized *Aicda*-Cre$^{+/ki}$ *R26tdTom*$^{+/ki}$ mice and single-cell sorted into 384-well plates filled with lysis buffer using an Aria III flow cytometric cell sorter and index sort option (BD Biosciences). RNA from single cells was retrotranscribed using random hexamer primers and cDNA was used as template for three independent nested PCRs with barcoded primers to amplify *Igh*, *Igk*, *Igl* transcripts. *Ighd*-specific primers were included in the Igh PCRs (1° PCR: mIghd-114-rv, 5′-CAGAGGGGAAGACATGTTCAACTAT-3′; 2° PCR: mIghd-079-rv, 5′-CAGTGGCTGACTTCCAATTACTAAAC-3′). Amplicons were pooled and sequenced on Illumina MiSeq 2 × 300 (Eurofins MWG) and data was processed and analyzed with sciReptor version v1.1-2-gf4cf8e2 (Imkeller et al., 2016).

Enzyme-linked immunosorbent assay (ELISA) for immunoglobulin detection

Total, MDA-LDL- and MDA-BSA-specific IgG and IgM antibody titers in plasma or serum were determined using mouse IgM, mouse IgG, mouse IgG1, mouse IgG2b and mouse IgG2c ELISA Quantitation Kits or antibodies (Bethyl laboratories; E90-101, E90–131, A90-105P, A90-109P, A90-136P, respectively) used in accordance with the manufacturer's instructions. In brief, plates were coated with goat anti-mouse IgM or IgG capture antibodies, MDA-LDL (3 μg/mL) or MDA-BSA (5 μg/mL) overnight at 4°C. Then, plates were blocked and incubated with diluted plasmas (1/50 for IgM, 1/20 for IgG and 1/20000 for IgG1, IgG2b and IgG2c). Goat anti-mouse IgM, IgG, IgG1, IgG2b or IgG2c detection antibodies conjugated to HRP followed by TMB substrate solution (Bethyl laboratories, E102) were added to the plate and finally measure the absorbance at 450 nm. For competition immunoassays, pooled plasma (1/20000 dilution) from MDA-LDL + CFA immunized mice was preincubated with increasing concentrations (0, 25, 50, 100, 150, 200 and 300 μg/mL) of the indicated competitors (BSA, MDA-BSA, LDL and MDA-LDL) overnight at 4°C. Plasma-competitor solutions were then centrifuged at 15.800 g for 45 min at 4°C. Supernatants were added to MDA-LDL coated (3 μg/mL) ELISA plates after blocking. IgG1 bound antibodies from plasma were detected by adding a goat anti-mouse IgG1 detection antibody conjugated to HRP followed by the addition of TMB substrate solution. Results were expressed as ratios of IgG1 binding to MDA-LDL in the presence (B) or absence (B_0) of the competitor.

Quantification of atherosclerosis progression

Perfused hearts were fixed with 4% PFA 2 h at RT, incubated with 30% sucrose overnight, embedded in OCT compound (Sakura, 4583) and frozen using dry ice. Subsequently, aortic sinus was sectioned from proximal aorta to heart apex using a cryostat (10 μm sections). Atherosclerosis extent was evaluated by quantifying atherosclerotic plaque area in five to six serial 80 μm-spaced aortic sinus cross sections stained with Oil-Red-O. Mayer's Hematoxylin (Bio-Optica, 05–06002/L) was used for nuclear counterstaining, and images were acquired with a DM2500 microscope (Leica). Image quantification was performed with Image J software (Venegas-Pino et al., 2013). Area under the curve (AUC) analysis of quantified atherosclerosis value of Oil Red-O-stained serial 80 μm-spaced aortic sinus cryosections was performed using GraphPad Prism (version 7.03 for Windows, GraphPad Software, La Jolla California USA, www.graphpad.com). To normalize the AUC of *Prdm1*$^{+/+}$ or *Prdm1*$^{fl/fl}$ MDA-LDL + CFA and CFA groups to PBS, the AUC value of each mice was divided by the mean AUC of the PBS group with the same genotype (*Prdm1*$^{+/+}$ or *Prdm1*$^{fl/fl}$) and the result was multiplied by 100. Collagen content within atherosclerotic lesions was quantified from Picrosirius Red-stained cryosections and images were taken using ECLIPSE 90i microscope (Nikon). Plasma or serum lipid and lipoprotein (LDL cholesterol, HDL cholesterol, triglycerides and total and free cholesterol) profile from pooled or individual animals was measured using Dimension RxL Max Analyzer (Siemens).

Necrotic core analysis

For aortic sinus necrotic core analysis, heart cryosections were stained with hematoxylin-eosin (H&E). Stained were scanned with an Axio scan. Z1 (Zeiss). Images were exported with ZEN blue software. Image quantification was performed using Image J software.

Immunofluorescence

For GC immunofluorescence, C57/BL6 mice were immunized with a single shot of MDA-LDL and sacrificed 10 days after immunization. Lymph node and spleen cryosections were incubated with 20 mM NH_4Cl 10 min at RT. Sections were permeabilized and blocked with 0.3% Triton X-100 (Sigma-Aldrich, T9284-500mL) and 2% BSA for 1h at RT. Then, samples were incubated with anti-B220 (BD Bioscience) PNA (Life Technologies) and DAPI (Sigma-Aldrich, D9542) overnight at 4°C. Slides were mounted with Prolong Gold (Life Technologies, P36930). Images were taken using a Zeiss LSM 700 confocal microscope (Zeiss). For aortic sinus immunofluorescence, heart cryosections were incubated with 20 mM NH_4Cl 10 min at RT. Then, sections were permeabilized with 0.5% Triton X-100 (Sigma-Aldrich, T9284-500mL) in PBS 30 min at RT and blocked with 2% BSA and 5% Donkey Serum (Sigma-Aldrich, D9663) in PBS during 1 h at RT. Subsequently, Avidin/Biotin blocking kit (Vector Labs, SP-2001) was used to block endogenous biotin in the sample. Samples were incubated with commercial primary antibodies SMA-1 (1A4, ThermoFisher Scientific) and MAC-2 (M3/38, Cedarlane (TebaBio)) overnight at 4°C. After washing, Goat anti-rat-Alexa Fluor 568 and Streptavidin-Alexa Fluor 488 (ThermoFisher Scientific) were added to the sample and incubated for 1h at RT. Slides were mounted with Prolong Gold (Life Technologies, P36930) after DAPI staining and images were taken using a SPE confocal microscope (Leica). Image quantification was performed with Image J software.

QUANTIFICATION AND STATISTICAL ANALYSIS

Data are presented as means ± standard deviation (SD). Statistical analysis was performed in GraphPad Prism (version 7.03 for Windows, GraphPad Software, La Jolla California USA, www.graphpad.com). Normality of the data was assessed by D'Agostino & Pearson normality test. For data coming from a Gaussian distribution, two-tailed unpaired Student t-test (p value $\leq$0.05 was considered significant) was used when comparing two experimental groups, one-way ANOVA was used when comparing three experimental groups (p value $\leq$0.05 was considered significant after correcting by two-stage linear step-up procedure of Benjamini, Krieger and Yekutieli test) and two-way ANOVA was used when comparing two experimental groups along time (p value $\leq$0.05 was considered significant after correcting by two-stage linear step-up procedure of Benjamini, Krieger and Yekutieli test). When analyzing not normally distributed data, Mann Whitney test was used for analyzing two groups (p value $\leq$0.05 was consider significant) and Kruskal–Wallis test (p value $\leq$0.05 was consider significant after correcting for multiple comparison by two-stage.